UNIVERISTY OF PISA

MASTER'S DEGREE DISSERTATION

IN

TELECOMMUNICATION ENGINEERING

A NOVEL SIW CAVITY-BACKED CORK ANTENNA RECONFIGURABLE IN POLARIZATION THROUGH FEED-LINE BIAS

SUPERVISIORS:
PROF. DR. IR. PAOLO **NEPA**
PROF. DR. IR. GIULIANO **MANARA**
PROF. DR. IR. HENDRIK **ROGIER**

CANDIDATE:
ANTONIO **GENTILE**

COUNSELLORS:
IR. ANDREA **MICHEL**
IR. SAM **AGNEESSENS**
IR. SAM **LEMEY**

ANNO ACCADEMICO 2015/16

"If you want to find the secrets of the universe,
think in terms of energy, frequency and vibration."

Nikola Tesla

Preface

This master thesis was done in collaboration with the faculty of Engineering and Architecture at Ghent University, Belgium. In particular, I spent five months at the laboratories of the Information Technology Department of the mentioned university. The collaboration was sanctioned by an Erasmus grant for traineeship.

I would like to thank my promotor Prof. Dr. Ir. Hendrik Rogier for accepting my candidature and providing me this thesis subject. I am also thankful to my supervisior dr. Ir. Sam Agneessens and Ing. Sam Lemey, who were always willing to help me in my trouble.

UNIVERSITEIT GENT

CONTENTS

Glossary

AR Axial Ratio

AUT Antenna Under Test

CBPA Cavity Backed Patch Antenna

CP Circular Polarization

CST Computer Simulation Technology

DC Direct Current

EM Electromagnetic

FET Field-effect Transistor

FTBR Front-to-Back Ratio

IL Insertion Loss

IoT Internet of Things

LHCP Left Handed Circular Polarisation

LP Linear Polarization

MEMS Micro Electro-Mechanical Switches

MIMO Multiple Input Multiple Output

PCB Printed Circuit Board

PEC Perfect Electric Conductor

RHCP Right Handed Circular Polarisation

RF Radio Frequency

SIW Substrate Integrated Waveguide

UWB Ultra Wide Band

Chapter 1: Introduction

1.1 The Next Generation: Internet of Things

The internet and the next generation of wireless communications are currently converging towards the “Internet of Things” (IoT). Internet of things is the network of physical devices embedded with electronics, software and sensors that enables these objects to collect and exchange data. The far-reaching integration of everyday objects into the network is a key feature of this evolution.

1.2 Antenna Design Challenges

Antennas for IoT applications pose specific design challenges. First, given the expected growth of connected devices in the next years, these antennas should be low cost and have low power consumption to be used in different environments for different applications. Furthermore, they should be made of novel specific materials to be easily integrated into objects and hence should be low profile as well. Nevertheless high isolation between the antenna and its environment is required to avoid mutual interference between devices. Devices involved in Internet of things network should be able to change data at high rate. Thus the necessity to have an antenna with wide impedance bandwidth. Furthermore, an antenna reconfigurable can be useful for Internet of things applications because the same antenna topology can be used for different purposes. For instance, a frequency reconfigurable antenna can work in different frequency band and so can be used to control different devices. Or also, a polarization reconfigurable antenna can select the best polarization depending on the environment and/or on the transmitting polarization to achieve the best match and enhance the received signal level. Substrate Integrated Waveguide (SIW) cavity-backed slot antennas have been used to achieve the majority part of the requirements mentioned above.

1.2.1 Substrate Integrated Waveguide

The idea of substrate integrated waveguide originates from the combination of waveguide and microstrip. In building a complete RF system, both planar printed transmission lines

and traditional waveguides encounter the same integration problem. Active components, passive components and transmission components, usually, are made by different manufacturing methods and with different interfaces, thus extra losses are incurred during the insertion, transition, and transmission process. As a consequence, the ideal design performance for each system components cannot be achieved. In order to optimize the system integration, a novel guided structure called substrate-integrated-waveguide (SIW) has been put forward, as shown in Figure 1.1 (a). Moreover, the transmission lines formed by the SIW not only have the favorable physical characteristic of planar printed transmission lines, but also possess the excellent performance of solid waveguide.

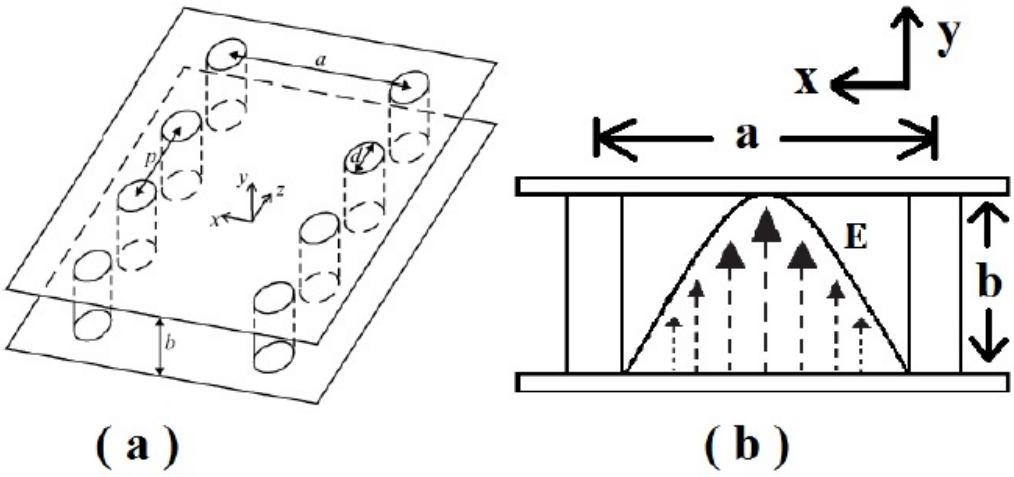

Fig. 1.1: (a) SIW structure of perspective view and (b) fundamental mode of SIW in cross-section view [16].

Essentially, the structure of SIW is similar to a rectangular-dielectric-filled waveguide structure. By adopting the PCB fabrication method of microstrip, SIW, however, scales down original height to the thickness of PCB. The PCB substrate, in this sense, can be regarded as the inner-filled dielectric of a waveguide. The two copper sheets of PCB are equivalent to the two metallic broad walls of waveguide. And the two rows of electroplated via holes, which drilling through the PCB, replace the narrow walls of waveguide. Therefore, the copper sheets and via holes form a current loop in the sectional view, which is similar to the cross-section case of traditional solid metal waveguide. In addition, all these via holes are drilled in equal distance, and the regular interval between

each pair of adjacent loops is in inverse proportion to the density of via holes. So that, the arrangement of via holes in PCB can form a complete dielectric-filled waveguide.

Similar to the propagation characteristic in bulky waveguide, the compressed electromagnetic wave in SIW also moves forwards along a zigzag route between the two rows of via holes by being reflected. Therefore, each SIW has a specific lowest transmission frequency. And the wavelength of the cut-off frequency should be in proportion to the width of the particular SIW. It is to be noted here that the most distinguishing mark of SIW is the current distribution on via holes. The surface current on a traditional waveguide can flow towards to any direction. But the current on via holes surface is limited to vertical direction. As individual via holes are discrete, the side wall current cannot flow longitudinally across the regular intervals. Therefore, the propagation in SIW can only perform TE_{m0} modes of traditional rectangular waveguide, in which the E-field is perpendicular to the propagation direction and will not change across the Y-axis. Thus, the first mode of SIW is the TE_{10} mode, as shown in figure 1.1 (b) [16]. Substrate – Integrated – Waveguide (SIW) cavity-backed antenna topologies exhibit many desirable properties for IoT application. They provide high radiation efficiency, good front-to-back ratio (FTBR) and high isolation from their surroundings, making them suitable for low power applications. Furthermore, their low profile allows for integration into floor and wall materials [2].

1.2.2 SIW Application and Device

The SIW not only realize the same function as solid waveguides do, but also can achieve some system functions of RF front-end circuitry, such as power amplifier, mixer, power divider, phase shifters, magic-T, directional couplers and circulators. As one of the necessary active devices in RF circuit is the oscillator, the oscillator for planar SIW attracts much attention. The major research interests about SIW passive devices focus on filters. This is because the design work of SIW devices is simplified from a traditional solid design to a two-dimensional design. As the visible side walls in SIW can be used as reference, additional via holes can be precisely inserted at target points. Moreover, as SIW devices are in planar form, all these designs can be either integrated in one single board or vertically stacked together [16].

1.2.3 Future Research Trends

The future activities on SIW technology will be mainly devoted to the deployment of mm-wave components in the frequency band between 60 and 350 GHz, to the investigation of new materials and fabrication technologies, and to the integration of complete systems in SIW technology based on the System-on-Substrate approach. Of course, the integration of SIW components other substrate integrated structures would be of great interest to design some innovative circuits systems.

The availability of SIW components in the frequency band said above, will open interesting perspective for novel applications and new markets. The technological development will permit to design novel compact and broadband components to meet the needs of UWB systems, scientific instrumentation, and low-cost commercial circuits for telecommunications. Among the possible components of practical interest, there are compact, high-order, bimodal filters for space applications, band-pass filters with very broad pass band for application in measurement instrumentation, six-port circuits for application to software-defined radio, circuits including active devices for radiometers at 35 and 94 GHz, diplexers and antennas for automotive radars at 77 and 94 GHz [17].

1.3 Goal

The aim of this master dissertation is to design a novel SIW cavity-backed antenna that exhibits a wide bandwidth. Moreover, it will be able to switch its polarization between right and left hand circular polarization by means P-i-N diodes properly biased applying a certain DC current on the coaxial feed cable together with the RF signal. This biasing techniques eliminates the need for an extra layer on top of the antenna for the biasing circuit and minimizes the amount and length of required cables, which both degrade the antenna performance. The merits of a reconfigurable design lie in the fact that the design can be generic. One design can achieve multiple goals by electrically changing the bias. Because of this, a reconfigurable antenna can lead to higher reliability [6].

Chapter 2: Literature Study

The first part of this chapter will discuss the state of the art and the literature study about the known reconfigurable techniques for antennas showing some applications. Then, an introduction about the main parameters of an antenna and how is possible get them is made.

2.1 State of the Art

Polarization reconfigurable antennas have received increasing attention in the last decade. They are sometimes called "*polarization agile antennas*", because they can alter their polarization characteristic in real time. This is a desirable feature for wireless applications as it doubles the system capacity through a frequency reuse, provides a powerful modulation scheme for microwave tagging systems, and becomes a candidate for multiple-input multiple-output (MIMO) systems. Therefore, they are useful for the compactness and light weight of wireless devices. Polarization switching can be established with the aid of switching devices such as PIN diodes or RF-MEMs. The design used in [18], depicted in Fig. 2.1, uses a P-i-N diodes to switch from linear polarization (LP) to circular polarization (CP) and from left handed circular polarization (LHCP) to right handed circular polarization (RHCP).

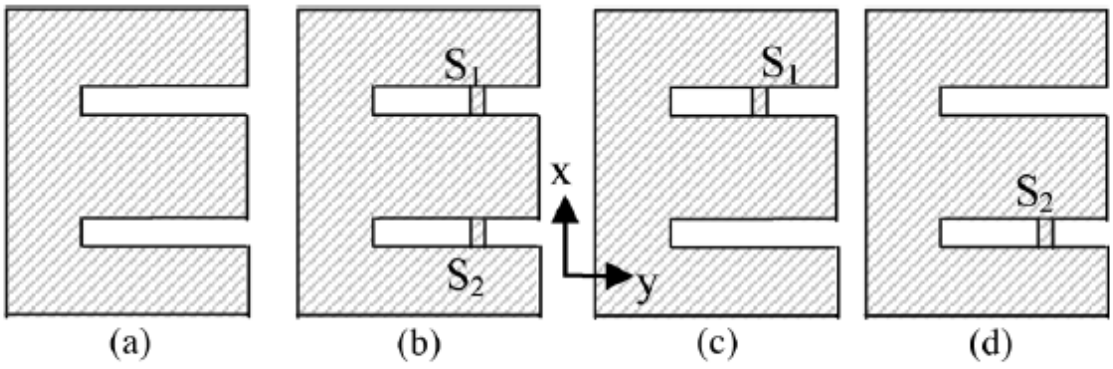

Fig. 2.1: a) LP state 1; b) LP state 2, c) LHCP state 3; d) RHCP state 4 [18].

The design depicted in Fig. 2.2 shows another way to achieve the polarization agility. The original orthogonal linear polarized antenna is a square patch fed by two ports at the adjacent edges. Circular polarization operations can be activated by introducing perturbations at the opposite corners of the patch. If a diode is loaded on every perturbed corner, the antenna polarization states can be alternated by controlling the bias voltage of two P-i-N diodes [28].

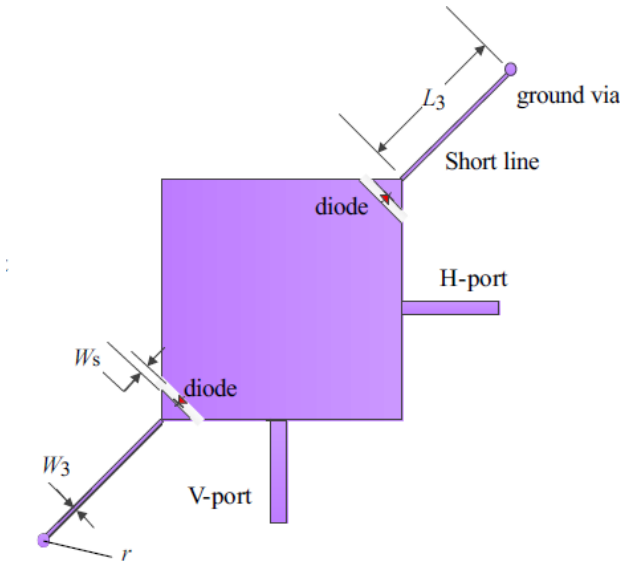

Fig. 2.2: Quad-Polarization Agile Antenna [28].

The geometry of a reconfigurable microstrip patch antenna with U-slot and truncated corners is illustrated in Fig. 2.3. Also in this case, the polarization diversity is obtained by turning three P-i-N diodes on the slot and the truncating corners of a square patch On and Off [29].

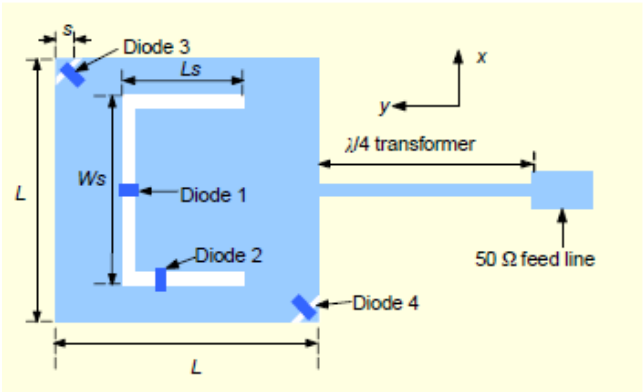

Fig. 2.3: Reconfigurable Microstrip Antenna with U-slot and truncated corners [29].

However, several problems still exist in these designs. In particularly the antennas mentioned above, and in general for the reconfigurable antennas, exhibit narrow bandwidth, complex design, and performance symmetry upon switching [18, 28, 29]. Furthermore, they need additional circuit for the biasing procedure, using wire and interconnections that could degrade the antenna performances. In this dissertation, an agile antenna able to switch between RHCP and LHCP using a novel techniques to bias the switching components in a huge frequency bandwidth around 3.5 GHz is investigated.

2.2 Polarization Reconfigurability

In order to create a reliable communication channel, diversity could be exploited making the antenna reconfigurable in polarization. Antennas with polarization reconfiguration can realize frequency reuse, which expands the capacity of communication systems. Polarization agility antennas can also alleviate the disadvantageous influence caused by multipath effects. The polarization agility is controlled by using P-i-N diodes with bias circuits [4].

In the following paragraphs, a brief discussion about what circular polarization is and how it is defined is made. Furthermore, it explains how we can recognize a right handed circular polarized wave from the left one and which components are suitable to switch between them.

2.2.1 Circular Polarization

In electrodynamics, circular polarization of an electromagnetic wave is a polarization in which the electric field of the passing wave does not change in strength but only changes direction in a rotary manner. The strength and direction of an electric field is defined by an electric field vector. In the case of a circular polarizes wave, the tip of the electric field vector, at a given point in space, describes a circle as time progresses. If the wave is frozen in time, the electric field vector of the wave describes a helix along the direction of propagation.

2.2.2 Left/Right handedness conventions

Circular polarization may be referred to as right-handed or left-handed, and clockwise or anti-clockwise, depending on the direction in which the electric field vector rotates. Unfortunately, two opposing historical conventions exist.

From the point of view of the Source

When using this convention, left or right handedness is determined by pointing one's left or right thumb away from the source, in the same direction that the wave is propagating, and matching the curling of one's fingers to the direction of the temporal rotation of the field at a given point in space. When determining if the wave is clockwise or anti-clockwise circularly polarized, one again takes the point of view of the source, and while looking away from the source and in the same direction of the wave's propagation, one observes the direction of the field's temporal rotation. This convention is in conformity with the Institute of Electrical and Electronics Engineers (IEEE) standard and as a result it is generally used in the engineering community.

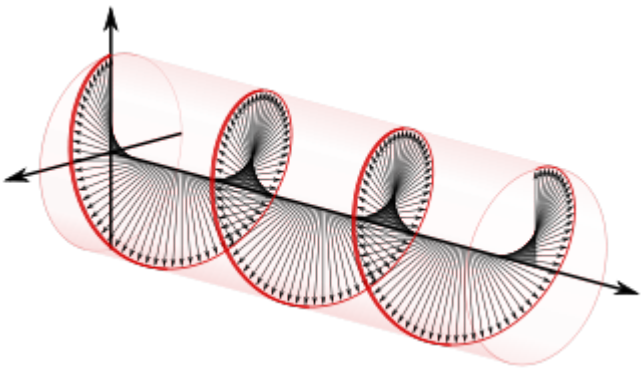

Fig. 2.4: Right-handed/clockwise circularly polarized light if defined from the point of view of the source.

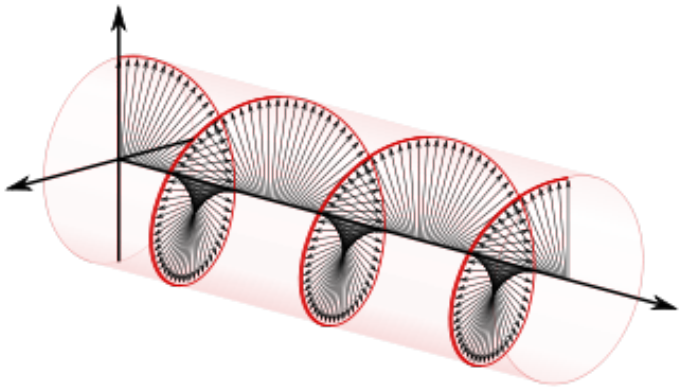

Fig. 2.5: Left-handed/counter-clockwise circularly polarized light if defined from the point of view of the source.

From the point of view of the Receiver

In this alternative convention, left or right handedness is determined by pointing one's left or right thumb toward the source, against the direction of propagation, and then matching the curling of one's fingers to the temporal rotation of the field.

When using this convention, in contrast to the other convention, the defined handedness of the wave matches the handedness of the screw type nature of the field in space. Specifically, if one freezes a right-handed wave in time, when one curls the fingers of one's right hand around the helix, the thumb will point in the direction which the helix progresses given that sense of rotation. Note that it is the nature of all screws and helices that it does not matter in which direction you point your thumb when determining its handedness.When determining if the wave is clockwise or anti-clockwise circularly polarized, one again takes the point of view of the receiver and, while looking toward the source, against the direction of propagation, one observes the direction of the field's temporal rotation.

2.3 Reconfigurable components

In order to make an antenna reconfigurable, its current distribution needs to be altered. The key challenge is to modify the current distribution in a useful way such that different states can be achieved.

To change the current on the antenna, a discrete switching element can be used. A switch is an electric component that connect or disconnect two parts of a circuit. Hence with a switch, two discrete states can be achieved, denoted as the "On-state" and the "Off-state". In the On-state an ideal switch can be interpreted as a zero resistance path while the Off-state can be modeled as a path with infinite resistance. Components that fit this description are Micro Electro-Mechanical Switches (MEMS), Field Effect Transistor (FET) and P-i-N diodes [6]. In this dissertation, P-i-N diodes are used for the antenna design. This section will explain the differences between the switching components mentioned above.

2.3.1 Fundamental Parameters

An important parameter is the operational frequency range of the component, which defines the frequency band in which the component will act reliably. Another one is the low profile in order to be as much as possible integrated with the planar geometry of the antenna. A last parameter that should be considered is the power consumption to have an efficient system.

Isolation

It is defined as the ratio of the output power in the On-state to the output power in the Off-state. It quantifies how good a switch is able to isolate two parts of a circuit while it is in the Off-state, relative to when it connects the two parts in the On-state [15]:

$$Isolation = 10 \log \frac{Pon}{Poff} \quad [\text{dB}]$$

Insertion Loss

The insertion loss (IL) of a component is defined as the ratio of the output power of the circuit with the component replaced by a short-circuit P_{sc} to the output power of the circuit with the switch in the On-state P_{on} [15]:

$$\text{IL} = 10 \log \frac{Psc}{Pon} \quad [\text{dB}]$$

The ideal switch has an IL of 0 dB. IL reduces the signal power and should therefore be as small as possible. These losses are mainly due to resistance losses, mismatch and/or transmission line loss.

Switching Speed

The switching speed is defined as the time that the component needs to switch from the On-state to the Off-state, characterized by the rise/fall time. The switching speed should be as high as possible.

2.3.2 Micro Electro-Mechanical Switches

The switch consist of an electrode and a suspended membrane. When an electric field is applied to the electrode, the membrane gets attracted and the switching action is complete. The merits of MEMS lie in the fact that these components have a low insertion loss, high isolation and near zero power consumption [12]. The disadvantages of this technology are the limited lifetime and the high actuation voltage (25-90V) to be able to switch [13]. For these reasons, this option is dismissed for this thesis in the future.

2.3.3 Field Effect Transistor

A FET is a device with three terminals: Drain, Gate and Source. The flow of radio frequency (RF) current between the source and the drain can be turned on or off by adjusting the bias voltage on the gate. The FET draws nearly no DC current in either the On or Off-state, giving it the advantage over some other switching components in terms of power consumption [12]. The isolation of FET degrades at higher frequencies (<10 dB) due to the effect of drain-to-source capacitance [14]. Moreover, a FET acting as a switch exhibits the highest IL of all discussed components. Hence, the dismissal of this component as switching element for the design.

2.3.4 P-i-N Diode

A P-i-N diode is a diode with a wide, undoped intrinsic semiconductor region between a p-type and an n-type semiconductor region. Two different bias states are available:

forward and reverse bias. A P-i-N diode is a current controlled component and acts as a variable resistor when forward biased. It makes for an excellent RF switch when it is forward biased, having a RF resistance around 1 Ω. When reverse biased, it acts as a small capacitance, such that, for the desired frequencies, it will act as an open switch. More details about the behavior of this component will be discuss in section 3.3.

2.3.5 Summary Table

	PRO	CONTRA
MEMS	+ Low insertion loss + High Isolation + Near zero power consumption + High linearity + Very high Q factor	- High actuation voltage - Delicate packaging - Limited lifetime - Slower switching speed
FET	+ Reliability + Simple bias + Low power consumption	- RF behavior - Highest insertion loss
P-i-N diode	+ High switching speed + Low package parasitic reactance + Small physical size + Good isolation at RF	- Insertion loss - Biasing circuit expensive - Highest power consumption

Table 2.1: Summary of the switchable components advantages and disadvantages.

2.4 Introduction to S-parameters

Figure 2.6 shows clearly how they are defined. The scattering matrix is a mathematical construct that quantifies how RF energy propagates through a multi-port network. For an RF signal incident on one port, some fraction of that signal gets reflected back out of the incident port, some of it enters into the incident port and then exits at (or scatters to) some or all of the other ports (perhaps being amplified or attenuated).

What's left of that incident power disappears as heat or even electromagnetic radiation. The S-matrix for an N-port contains N^2 coefficients (S-parameters), each one representing a possible input-output path. S-parameters are complex numbers, having real and imaginary parts or magnitude and phase parts, because both the magnitude and the phase of the incident signal are changed by the network.

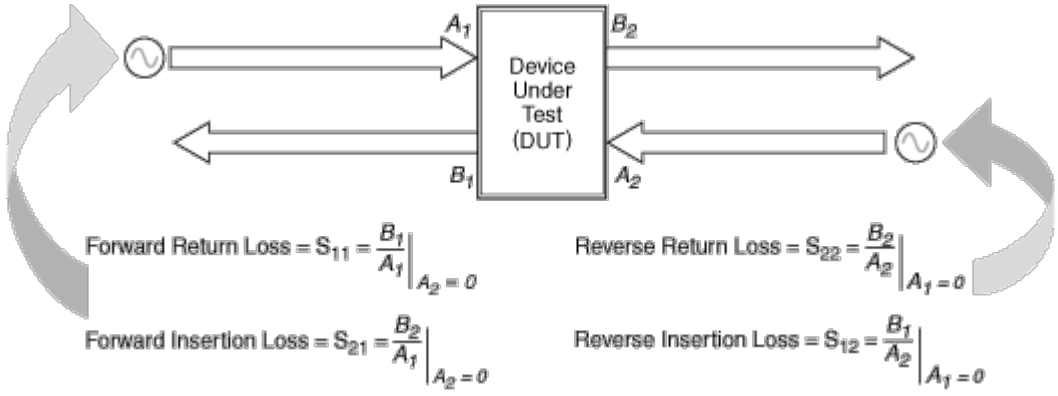

Fig. 2.6: S-Parameters Definition.

They are defined for a given frequency and system impedance, and vary as a function of frequency for any non-ideal network. S-parameters are usually displayed in a matrix format, with the number of rows and columns equal to the number of ports. For the S-parameter S_{ij} the *j* subscript stands for the port that is excited (the input port), and the *i* subscript is for the output port. Thus the S_{11} refers to the ratio of the amplitude of the signal that reflects from port one to the amplitude of the signal incident on port one. Parameters along the diagonal of the S-matrix are referred to as reflection coefficients because they only refer to what happens at a single port, while off-diagonal S-parameters are referred to as transmission coefficients, because they refer to what happens at one port when it is excited by a signal incident at another port.

2.4.1 S-parameters for Antennas

As said above, the S-parameters describe the input-output relationship between ports in an electrical system. A port can be loosely defined as any place where we can deliver voltage and current.

So, if we have a communication system with two radios (radio 1 and radio 2), then the radio terminals (which deliver power to the two antennas) would be the two ports. S_{11} then would be the reflected power radio 1 is trying to deliver to antenna 1. S_{22} would be the reflected power radio 2 is attempting to deliver to antenna 2. S_{12} is the power from radio 2 that is delivered through antenna 1 to radio 1.

In practice, the most commonly quoted parameter in regards to antennas is S_{11}. It represents how much power is reflected from the antenna, and hence is known as the *reflection coefficient* (or *return loss*). If it is equal to 0 dB, then all the power is reflected from the antenna and nothing is radiated. If it is equal to -10 dB, this implies that if 3 dB of power is delivered to the antenna, -7 dB is the reflected power. The remainder of the power was "accepted by" or delivered to the antenna. This accepted power is either radiated or absorbed as losses within the antenna. Since antennas are typically designed to be low loss, ideally the majority of the power delivered to the antenna is radiated.

For this reason, the antenna bandwidth is defined as the frequency range in which the S_{11} parameter is less than -10 dB.

2.5 Axial Ratio

The axial ratio is the ratio of orthogonal components of an E-field. A circularly polarized field is made up of two orthogonal E-field components of equal amplitude (and 90 degrees out of phase). Because the components are equal magnitude, the axial ratio is 1 (or 0 dB). Axial ratios are often quoted for antennas in which the desired polarization is circular. The ideal value of the axial ratio for circularly polarized fields is 0 dB. In general is common consider an antenna circularly polarized if its axial ratio is less than 3 dB (or 6 dB).

2.6 Antenna Radiation Pattern

The radiation pattern or antenna pattern is the graphical representation of the radiation properties of the antenna as a function of space. That is, the antenna's pattern describes how the antenna radiates energy out into space (or how it receives energy). It is important to state that an antenna radiates energy in all directions, at least to some extent, so the antenna pattern is actually three-dimensional.

It is common, however, to describe this 3D pattern with two planar patterns, called the principal plane patterns. These principal plane patterns can be obtained by making two slices through the 3D pattern through the maximum value of the pattern or by direct measurement. It is these principal plane patterns that are commonly referred to as the antenna patterns [26].

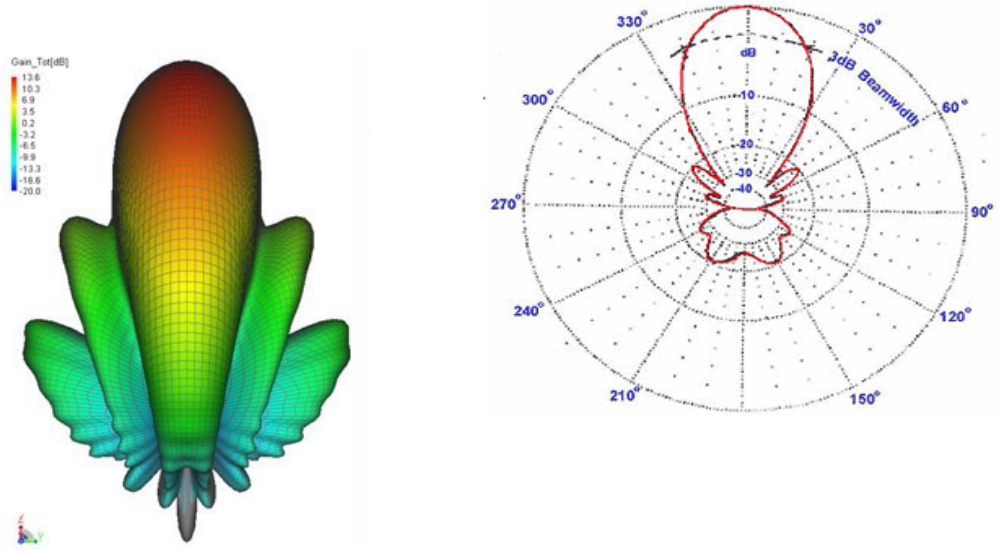

Fig. 2.7: Antenna's 3D-pattern (left) and 2D-pattern (right).

2.6.1 Required Equipment

For antenna test equipment, we will attempt to illuminate the test antenna, often called Antenna-Under-Test (AUT), with a plane wave. This will be approximated by using a source (transmitting) antenna with known radiation pattern and characteristics, in such a way that the fields incident upon the AUT are approximately plane waves [25]. The required equipment for antenna measurements include:

- The Transmitting System: it should be capable of outputting a stable known power. The output frequency should also be tunable (selectable), and reasonably astable, which means that the frequency you get from the transmitter is close to the frequency you want.

- The Receiving System: it simply needs to determine how much power is received from the test antenna. This can be done via a simple bolometer, which is a device for measuring the energy of incident electromagnetic waves.

- The Positioning System: it controls the orientation of the test antenna. Since we want to measure the radiation pattern of the AUT as a function of angle, we need to rotate the test antenna so that the source antenna illuminates the test antenna from different angles. The positioning system is used for this purpose.

Once we have all the equipment we need, we will nee to place it and perform the test in an antenna range, as explained in the next section.

2.6.2 Free Space Ranges

Free space ranges are antenna measurement locations designed t simulate measurements that would be performed in space. That is, all reflected waves from nearby objects and the ground (which are undesirable) are suppressed as much as possible. The most popular free space ranges are: *anechoic chamber, elevated ranges* and the *compact range.* For this dissertation, the anechoic chamber will be used to perform the test.

2.6.3 Anechoic Chamber

Anechoic chambers are indoor antenna ranges. The walls, ceilings and floor are lined with special electromagnetic wave absorbing material. Indoor ranges are desirable because the test conditions can be much more tightly controlled than that of outdoor ranges. The material is often jagged in shape as well, making these chambers quite interesting to see. The jagged triangle shapes are designed so that what is reflected from them tends to spread in random directions, and what is added together from all the random reflections tends to add incoherently and is thus suppressed further. The drawback to anechoic chambers is that often need to be quite large. Often antennas need to be several wavelengths away from each other at a minimum to simulate far-field conditions. Hence, it is desired to have anechoic chambers as large as possible, but cost and practical constraints often limit their size.

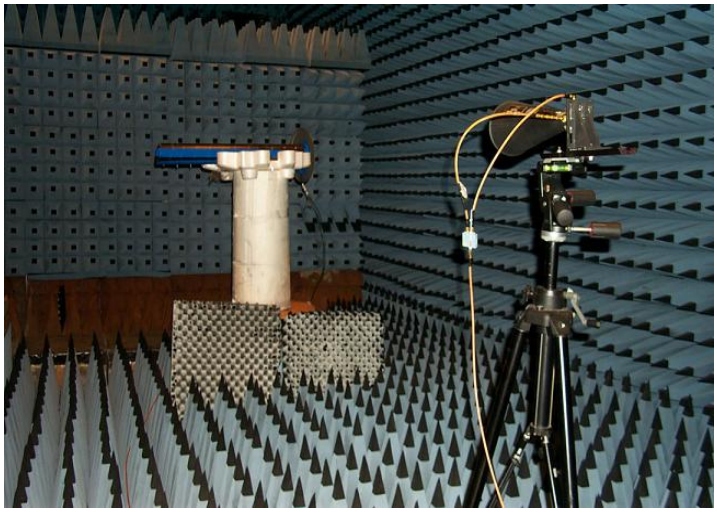

Fig. 2.8: Anechoic Chamber with some test equipment.

Universities with anechoic chambers typically have chambers that are 3-5 meters in length, width and height. Because of the size, and because RF absorbing material typically works best at UHF and higher, anechoic chambers are most often used fro frequencies above 300 MHz. Finally, the chamber should also be large enough that the source antenna's main lobe is not in view of the side walls, ceiling or floor [25].

2.6.4 Measurements Technique

The basic pattern-measurement technique that most people are familiar with, uses a single-axis rotational pattern. This technique involves an AUT placed on a rotational positioner and rotated about the azimuth to generate a two-dimensional polar pattern. This measurement is commonly done for the two principal axes of the antenna to determine antenna parameters. Figure 2.9 shows a typical polar-pattern test setup.

The AUT is placed on a rotating turntable, and a dual-polarized antenna is placed level with the AUT a fixed distance away. The turntable is rotated 360°, and the response between the antennas is measured as a function of angle.

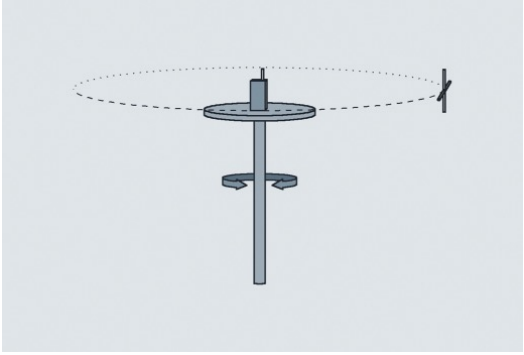

Fig. 2.9: Test setup for single-axis polar pattern measurement.

To generate a full spherical-pattern measurement, it is necessary to change the relationship between the AUT and the transmitting antenna and repeat the previous polar test for each new orientation. The changes in orientation must be perpendicular to the plane of measurement to completely cover a spherical surface. In simpler terms, the second axis of rotation must be perpendicular to and intersect the first axis of rotation [27].

2.7 Conclusion

The literature study showed that the P-i-N diodes are the components most used as switching components. The axial ratio bandwidth is defined as the frequency range in which the axial ratio is lower than 3 dB but, depending on the applications, also 6 dB could be acceptable.

Chapter 3: Design

3.1 Goal

The goal is to design an ultra-wideband (UWB) polarization reconfigurable Substrate Integrated Waveguide (SIW) cavity-backed antenna, centered around 3.5 GHz. The International Telecommunication Union Radiocommunication Sector (ITU-R) currently define UWB as an antenna transmission for which emitted signal bandwidth exceeds the lesser of 500 MHz or 20% of fractional bandwidth. The polarization must switch between right handed circular polarization and left handed circular polarization by means of P-i-N diodes properly biased.

3.2 Topology

The basic topology is depicted in Fig. 3.1. It consists of a main probe-fed patch and two parasitic patches, backed by a Substrate Integrated Waveguide (SIW) cavity. The conducting patches on the top are connected with the ground plane through vias in order to form a cavity. The vias are realized by brass eyelets (outer diameter $d=4mm$), spaced closely enough to minimize radiation loss [7]. Depending on the diodes biasing, it is possible to have two resonant structures: a half-mode and a quarter-mode resonator. By switching the diodes in the right state, we can choose which two quarter-modes combine to work as a half-mode cavity, while the other one acts as a stand-alone quarter mode.To achieve this, the feed point must be on the diagonal of the antenna, to maintain the symmetry. The main cavity and the parasitic ones have different size therefore they will have different resonance frequencies. If these frequencies are close each other, the ultra-wideband condition is achieved.

3.2.1 Main probe-fed Quarter Mode Cavity

The main resonant structure of the antenna is a square quarter mode cavity of L_p x W_p millimeters. In CST, it has been modeled as a PEC material. The ground plane is made of PEC as well. This quarter mode cavity is connected directly to the coax cable.

As said before, to achieve the reconfigurability the feed point must be on the diagonal of this cavity and, hence, of the antenna. In this design, the chosen feed point has coordinates ($feed_x$, $feed_y$), with $feed_x$ = 12 mm and $feed_y$ = - $feed_x$.

3.2.2 Parasitic Cavities

As said in section 3.2, parasitic cavities are needed to have two different resonant structures and hence to achieve the circular polarization condition, depending on the P-i-N diodes state. These cavities are separated by H_{slot} millimeters from the main cavity and they are not connected to the feed cable. Furthermore they are larger than the main cavity by an offset of 1 mm. This means that there is a coupling between the main cavity and these cavities. Actually, the only connection among them are the P-i-N diodes. When the P-i-N diode is forward biased, it work as an electric short and the current can flow from the main cavity to the respective parasitic cavity. In the same time, the other P-i-N diode is reverse biased and it works as an open circuit. This means that the respective parasitic cavity is isolated from the main cavity.

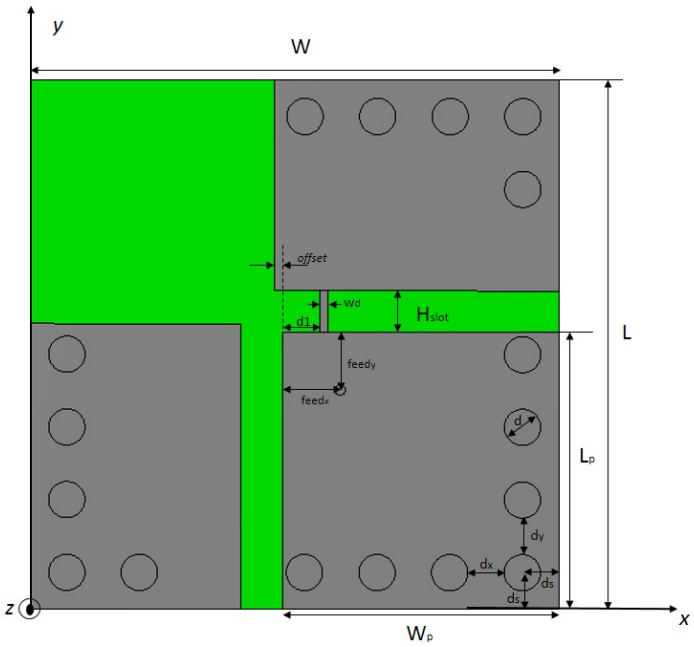

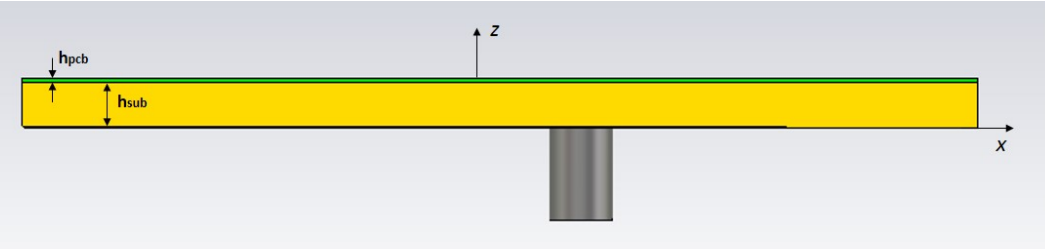

Fig. 3.1: Ideal components antenna design: top (up) and transversal (down) view.

Parameter	*Value (mm)*	*Parameter*	*Value (mm)*
W	64	H_{slot}	5
L	64	d_1	4.5
offset	1	w_d	1
W_p	33.5	$feed_x$	7
L_p	33.5	$feed_y$	- 7
h_{sub}	3	h_{PCB}	0.25
ε_{r_cork}	1.23	δ_{cork}	0.0263
ε_{r_PCB}	3.45	δ_{PCB}	0.0031
d	4	d_s	4.4
d_x	4.4	d_y	4.4
$feed_{in}$	1.3	$feed_{out}$	4.3

Table 3.1: parameter values for the design with ideal components.

3.2.3 Materials

As said before, a cork material is used as antenna substrate. Cork material is finding increasing application as an insulator in various fields including space technology, due to characteristic properties such as light weight and low thermal conductivity [8]. Furthermore, as cork is a common floor and wall material, the proposed low-profile antenna may unobtrusively be integrated into floors or walls [1].

A composite cork agglomerate by Amorim Cork Composites S.A., made of cork granules bound by polyurethane, with a density of 0.145 g/cm^3 and a thickness of 3 mm, is applied as antenna substrate. The cork characterization is discussed in [2]. For the CST simulations, the design is performed using the parameters ε_r = 1.23 and δ = 0.0263 determined at 3.5 GHz. Pure copper polyester taffeta fabric has been used as ground plane. It is characterized of 0.08 mm thickness, light weight (80 g/m2), flexible and easy to cut [31].

3.3 P-i-N Diodes

As a switching element, a P-i-N diode has been chosen. The P-i-N diode used in this thesis is the MA4AGBLP912 because of its low forward resistance and low capacitance value reverse biased state [9]. A diode needs to be biased by a current source. The biased circuit is based on a circuit made in another thesis [10]. With this circuit, bias current values ranging from 0-20 mA can be set. Considering that the main patch is connected to the ground plane, several capacitors within a tiny slot carved in the main patch are needed to avoid a short circuit. These capacitances must be properly chosen in order to block the DC required to polarize the diodes. The capacitors used in this thesis are the model 0402 of [11].

3.3.1 Biasing

Switching elements need to be biased in order to achieve different states. Hence, the need for a biasing circuit arises. Usually, this is done using an extra layer on the top of the antenna surface but this degrades the antenna performance. Also, the DC bias signal needs to be supplied to the biasing circuit separately from the RF signal. This is done using extra wires, which reduce the reliability. As stated in [10], the position of the biasing circuit in the layout is extremely important. The path for the RF signal should be as short as possible in order to reduce the global inductance of the circuit. Also, the length of the signal lines has to be much shorter than the wavelength to consider components as lumped.

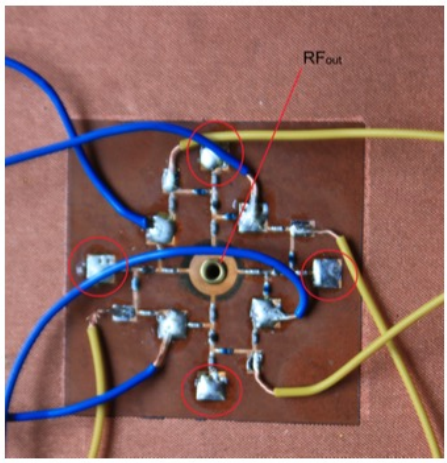

Fig. 3.2: Biasing circuit on the top layer structure.

An alternative approach will be used in this thesis. Instead of providing an extra layer and supplying a DC signal to this layer, the DC signal is directly fed to the antenna, reducing the total interconnections needed. This is done by superimposing RF and DC, using a bias tee on the inner conductor. The outer conductor of the coaxial cable is connected to the ground plane. The main advantage of the biasing method is the simplicity. The disadvantage of this techniques is that not all topologies are eligible. However, by paying extra attention to the topology during the design, this advantage can be completely omitted. These solutions will be discussed in the following chapters.

3.3.2 Bias Tee

A bias tee is a three port network that can be used for setting the DC bias point and forms an intricate part of the design. An equivalent circuit of a bias tee is depicted in Fig. 3.3. Its principle of operation can be viewed as an ideal capacitor that allows RF through but blocks the DC bias and an ideal inductor that blocks RF but allows DC.

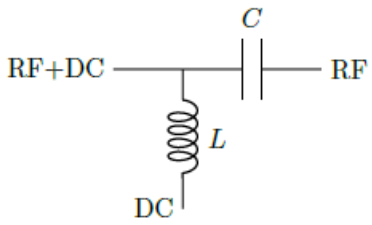

Fig. 3.3: Equivalent circuit of bias tee.

The capacitance value *C* is chosen such that the impedance of the capacitor is much smaller than the characteristic impedance, this is typically 50 Ohm, so it forms a low impedance path for RF signals

$$X_c = \frac{1}{j2\pi fC} << 50\ \Omega$$

The inductance value *L* is chosen such that the impedance of the inductor is much larger than 50 Ohm for any frequency of interest. This way, the path for the DC bias signal is short circuited, while it forms an high impedance path for the RF signals:

$$X_L = j2\pi fL >> 50\ \Omega$$

For the measurements of the antenna design, the bias tee of the Agilent network analyzer will be used. It uses wide band bias tee with are considerably more complicated than the simple model described above. However, the model is satisfactory over the complete bandwidth of interest of the design.

3.3.3 Bias Current Source

To bias a P-i-N diode, a current source has to be used. In the dissertation, the current source designed in a previous thesis [10] is reused. These are not readily available as voltage sources, so a biasing circuit needs to be created. It is based on the LM334 [24], a 3-terminal adjustable current source depicted in figure 3.4, in which I_{set} is completely determined by means of an external resistor R_{set} according to following relation:

$$I_{set} = I_{bias} + I_r = \frac{Vr}{Rset} + I_{bias}$$

I_{bias} is normally a small fraction of I_{set}, so the previous can be reduced to:

$$I_{set} = \frac{Vr}{Rset}\frac{n}{n-1}$$

with n the ratio of I_{set} to Ibias. This ratio can be approximated as n=18 when $2\mu A \leq I_{set} \leq 1$ mA.

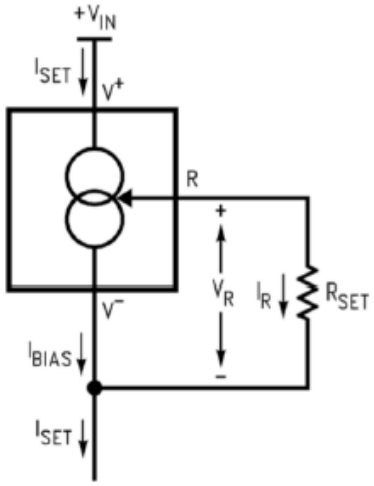

Fig. 3.4: LM334 current source schematic.

Therefore:

$$I_{set} = \frac{Vr}{Rset}\ 1.059 = \frac{227\ \mu V/K}{Rset}$$

This equation clearly shows that the desired current value can be set by selecting the correct value of R_{set}. The electrical circuit of Fig. 3.4 has been realized and it is shown in Fig. 3.5. It also has two switch to change the current polarity, and then the state of the diodes, without disconnect the cables.

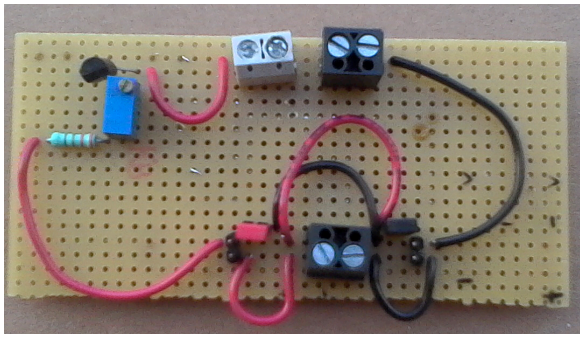

Fig. 3.5: Diodes Biasing Circuit.

3.3.4 Forward Bias

In the ideal model, the diode can be represented as a perfect short circuit. This is just an idealization of the model and it is needed to compare the results obtained in both cases. In the electric equivalent circuit model, instead, the diode will behave as a current controlled resistor, with a resistance R_s that depends on the forward current. This value can be found in the datasheet [9]. A higher current leads to a better matching until a certain point, after which this effects saturates.

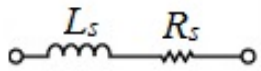

Fig. 3.6: Forward biased P-i-N diode equivalent circuit.

3.3.5 Reverse Bias

In the electric equivalent circuit model, when the diode is reverse biased by applying a negative voltage over the terminals, it will behave as a RC parallel circuit. The values for C_t and R_p can be found in the datasheet [9] and will depend on the applied reverse voltage. At high frequency, the magnitude of the bias voltage has a little effect on the capacitance value. The ideal model is a perfect open circuit. Actually, in both real case, there is a parasitic inductance L_s in series. The inductance value depends on the package size.

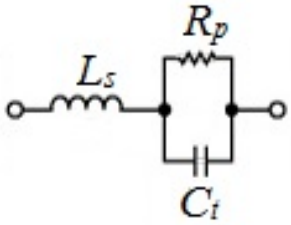

Fig. 3.7: Reverse biased P-i-N diode equivalent circuit.

3.5 Simulations & Results

In the next paragraphs, the simulations results are shown. First, a brief introduction to CST Microwave Studio, then the definition of the two design for different components and the relative results.

3.5.1 Introduction to CST

CST Microwave Studio is a specialist tool for the 3D EM simulation of high frequency components and devices such as antennas, filters, couplers, planar and multi-layers structures. CST Microwave Studio integrated time domain and frequency domain full-wave algorithm to solve Maxwell equations for planar circuits. In this thesis, the frequency domain solver is selected.

3.5.2 Antenna with Ideal Components

The design is depicted in Fig. 3.8. In this case, to don't take in account the effects of the lumped components, they are represented ideally. In particular, the forward biased P-i-N diode is represented as a metal strip (perfect short circuit) while the reverse biased P-i-N diode is a perfect open circuit.

That's the way there isn't in the following design. The DC capacitors blocker are not take in account as well. For the ideal components antenna design, the parameters values are the same shown in Table 3.1.

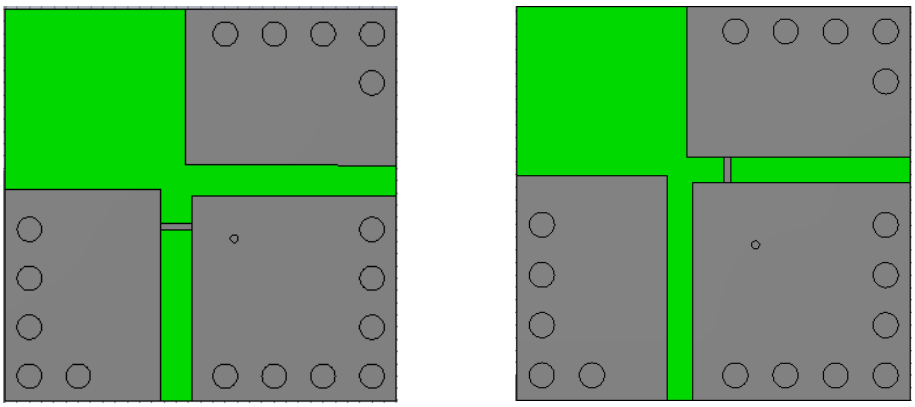

Fig. 3.8: LHCP (on the left) and RHCP (on the right) Antenna with ideal components.

Right Hand Circular Polarization

In this configuration the antenna acts as a *vertical* half-mode cavity and results right handed circular polarized. The design top view is shown in Figure 3.8.

In the figures below, the results for this case are shown.

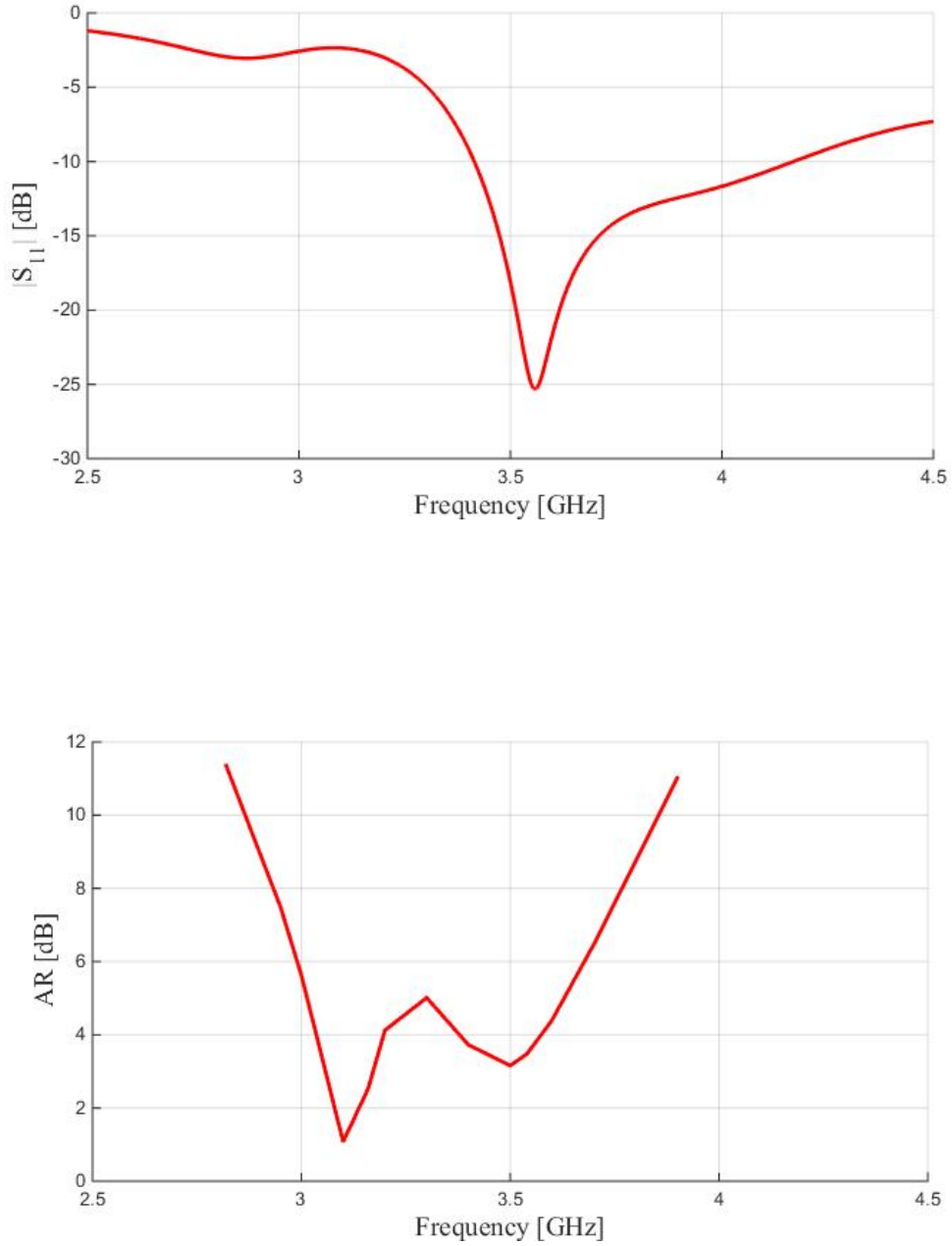

Fig. 3.9: S_{11} (up) and Axial Ratio (down).

Left Hand Circular Polarization

In this case, the design changes only for the diode position that now it is positioned in the vertical slot. The antenna is symmetric along the diagonal.

In the figures below, the results for this case are shown.

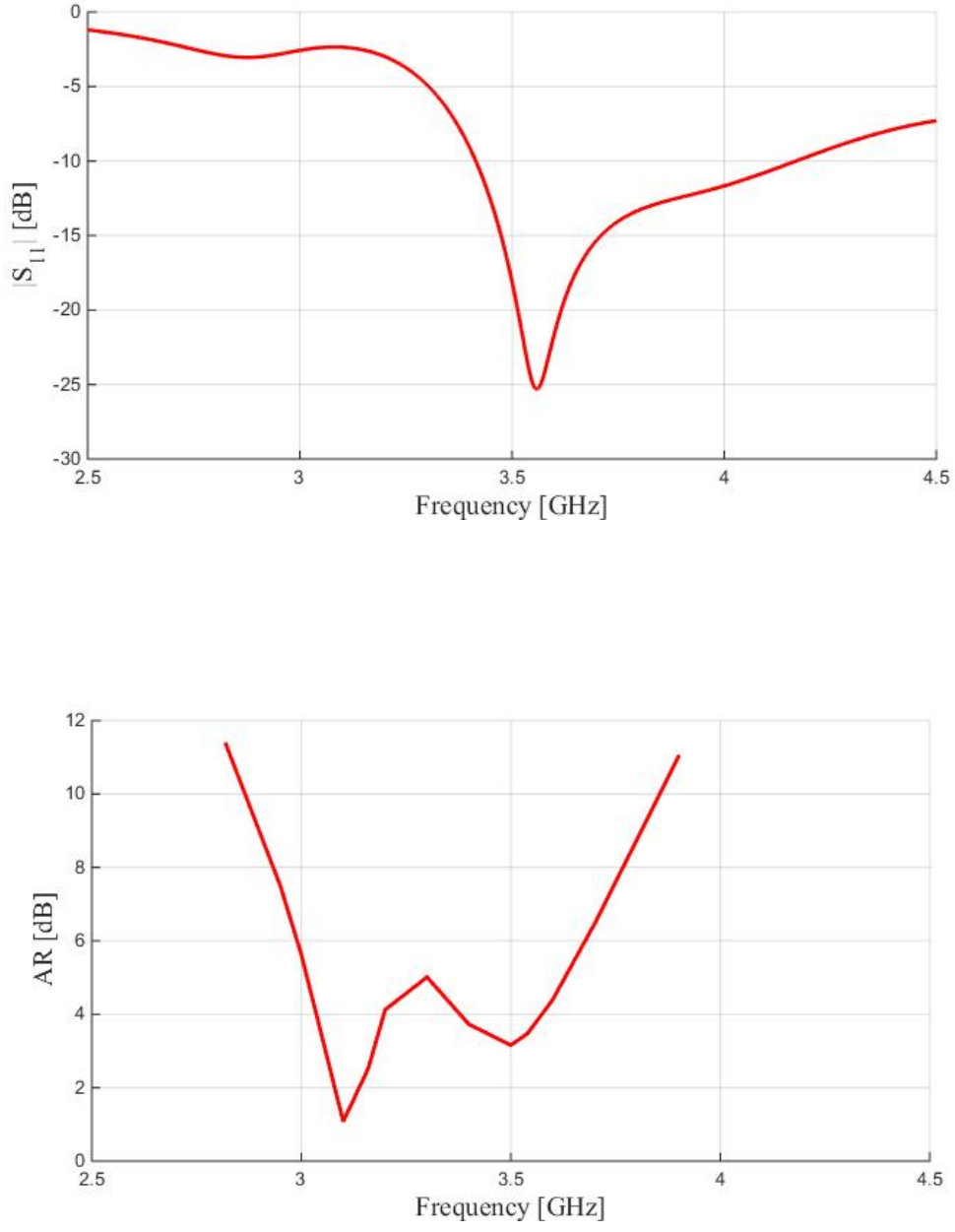

Fig. 3.10: S_{11} (up) and Axial Ratio (down).

In-Depth Study

As said in section 3.2.3, cork is a non homogeneous material. Thus, a parametric simulation, varying the cork dielectric properties around the chosen value in 3.2.3 (which is the average value), has been made to see the influence on the antenna parameters. As we can see from the results shown in the next picture, there are little variation of the parameters. Hence the antenna structure can be considered quite stable to the cork's dielectric properties.

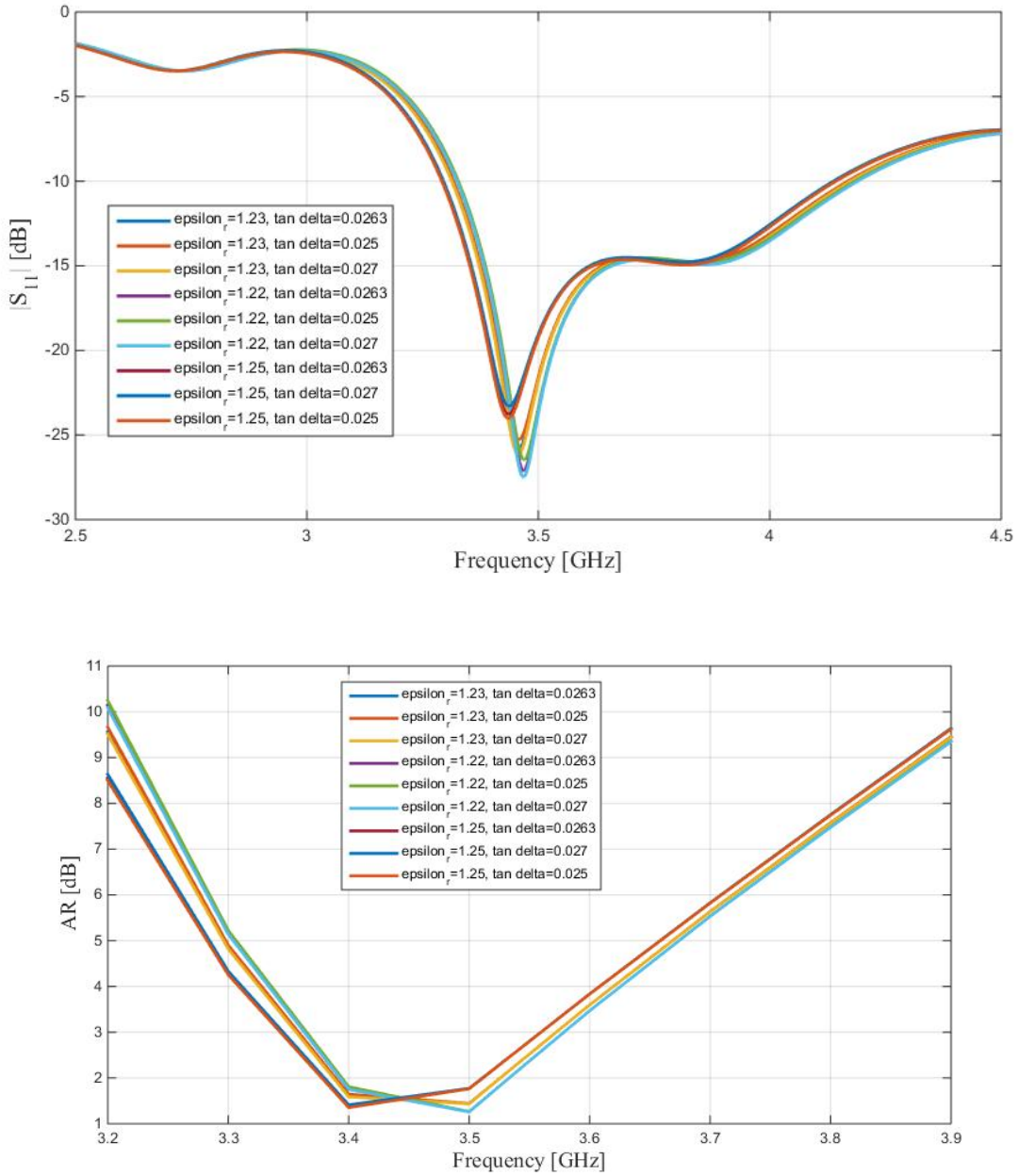

Fig 3.11: Parametric Simulation Study.

Simulating the model in a larger frequency range, it is possible to see a third mode excited at 5 GHz, how shown in Figure 3.12. How we can see, the third mode is excited but it is not very well matched to the 50 Ohm input impedance. We will use it to achieve more bandwidth in the design with lumped components, as explain in section 3.5.5. The extra mode is due to the fact that the parasitic elements radiate, at that frequency, from their edges. This behavior is shown in Figure 3.13.

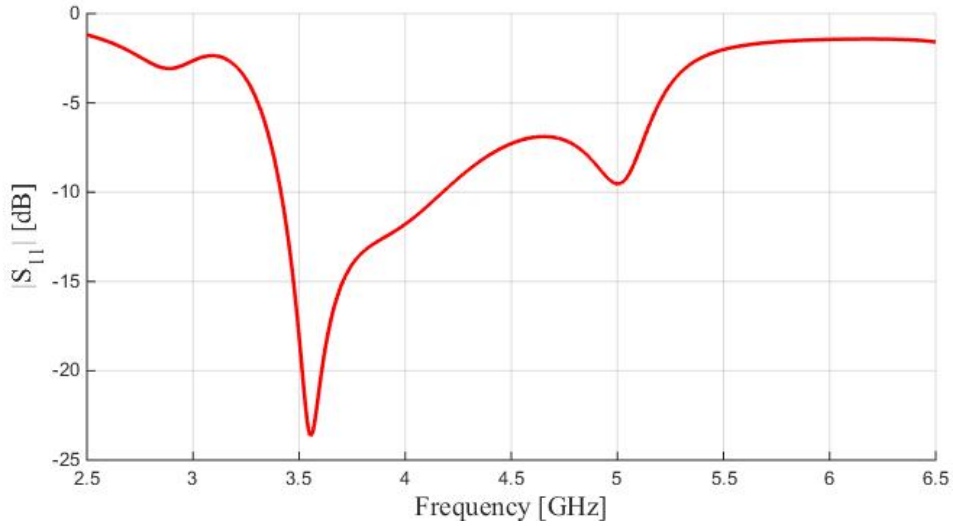

Fig. 3.12: S11 in a larger frequency range.

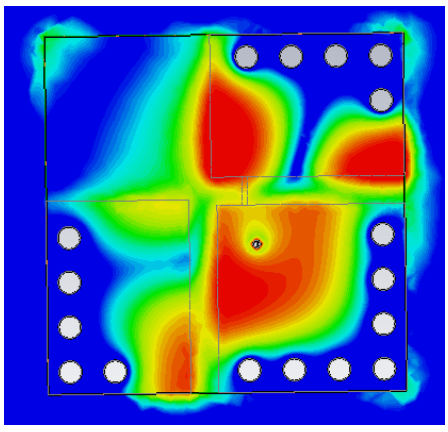

Fig. 3.13: Absolute E-Field at 5 GHz.

3.5.3 Antenna with Lumped Components

To be able to polarize the P-i-N diodes, DC capacitors are used and their effect is taken in account for CST simulations. Also the P-i-N diodes effects are taken in account during the simulations. As said in section 3.3, they are represented as a low resistance when it is forward biased and as a R-C parallel circuit when it is reverse biased. In both cases, they have a inductance in series that depends by the package.

3.5.4 Design Improvements

Traditional probe-fed CP patch antennas are attractive design candidates due to their simplicity and intuitive design strategy, but unfortunately they suffer from narrow axial ratio (AR) and S11 bandwidths (< 2%) [30]. To achieve the required specifications, some solutions have been found out.

3.5.5 Bandwidth Improvement

As we can see in fig. 3.9 and 3.10, there is a mismatch between the impedance and the axial ratio bandwidth. This is due to the feed reactance. By integrating an annular gap capacitor is possible to compensate the probe reactance and achieve a better matching between the two bands. The annular gap capacitor has width of 0.1 mm and radius of 7 mm. Furthermore, the lumped components have a negative effects on the impedance bandwidth. Hence, we exploited the third mode, discussed in *In Depth Study* section, to achieve a huge bandwidth.

3.5.6 Polarization Improvement

Due to the fact that the antenna is very sensitive to variations in the geometry, it was decided to print the patches on a PCB layer. This is I-Tera 0.25 mm layer and it should be considered in the CST model. Furthermore, a structure connected to the ground plane through vias has been added to reduce the radiation effects from the edges of the parasitic patches that could influence the polarization pattern. The final design and the relative parameters values are shown in Figure 3.14 and Table 3.2.

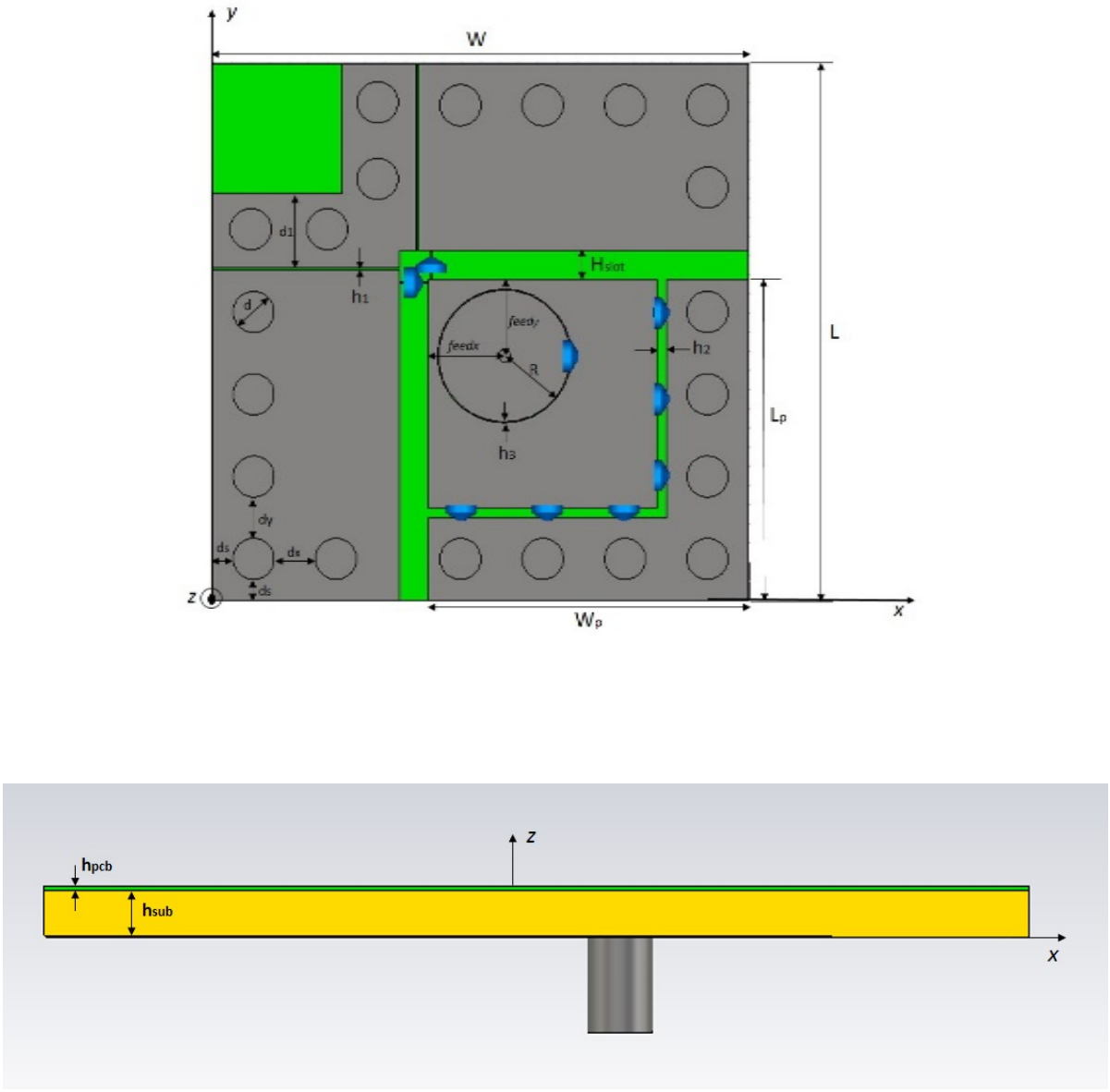

Fig. 3.14: Lumped components Antenna Design: top (up) and transversal (down) view.

Parameter	*Value (mm)*	*Parameter*	*Value (mm)*
W	54	H_{slot}	5
L	54	d	4
W_p	33.5	$feed_x$	7
L_p	33.5	$feed_y$	- 7

h_{sub}	3	h_{PCB}	0.25
ε_{r_cork}	1.23	δ_{cork}	0.0263
ε_{r_PCB}	3.45	δ_{PCB}	0.0031
d	4	d_s	4.4
d_x	4.4	d_y	4.4
$feed_{in}$	1.3	$feed_{out}$	4.3
R	7	d_1	7.75
h_1	0.25	h_2	1
h_3	0.1		

Table 3.2: Parameter values for the lumped components antenna design.

3.5.7 Additional Changes

As it is possible to see in [9], the diode length is less than 1 mm while the slot width is 3 mm. Hence, in order to solder them, a particular foot print has been added. Its best position was found by simulation and it is 0.2 mm large, 1.2 mm long and 0.25 mm away from the main patch edge. For this reason, the diodes, depicted in blue in Fig. 3.15, were soldered in a reflow oven. The following figure shows the structure details.

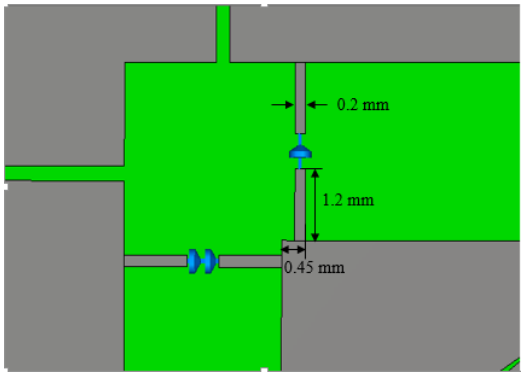

Fig. 3.15: Diodes support structure.

Right Hand Circular Polarization

For this case, due to the lumped components effects, the solutions discussed in section 3.4 have been introduced and the design is the same of Fig. 3.14.

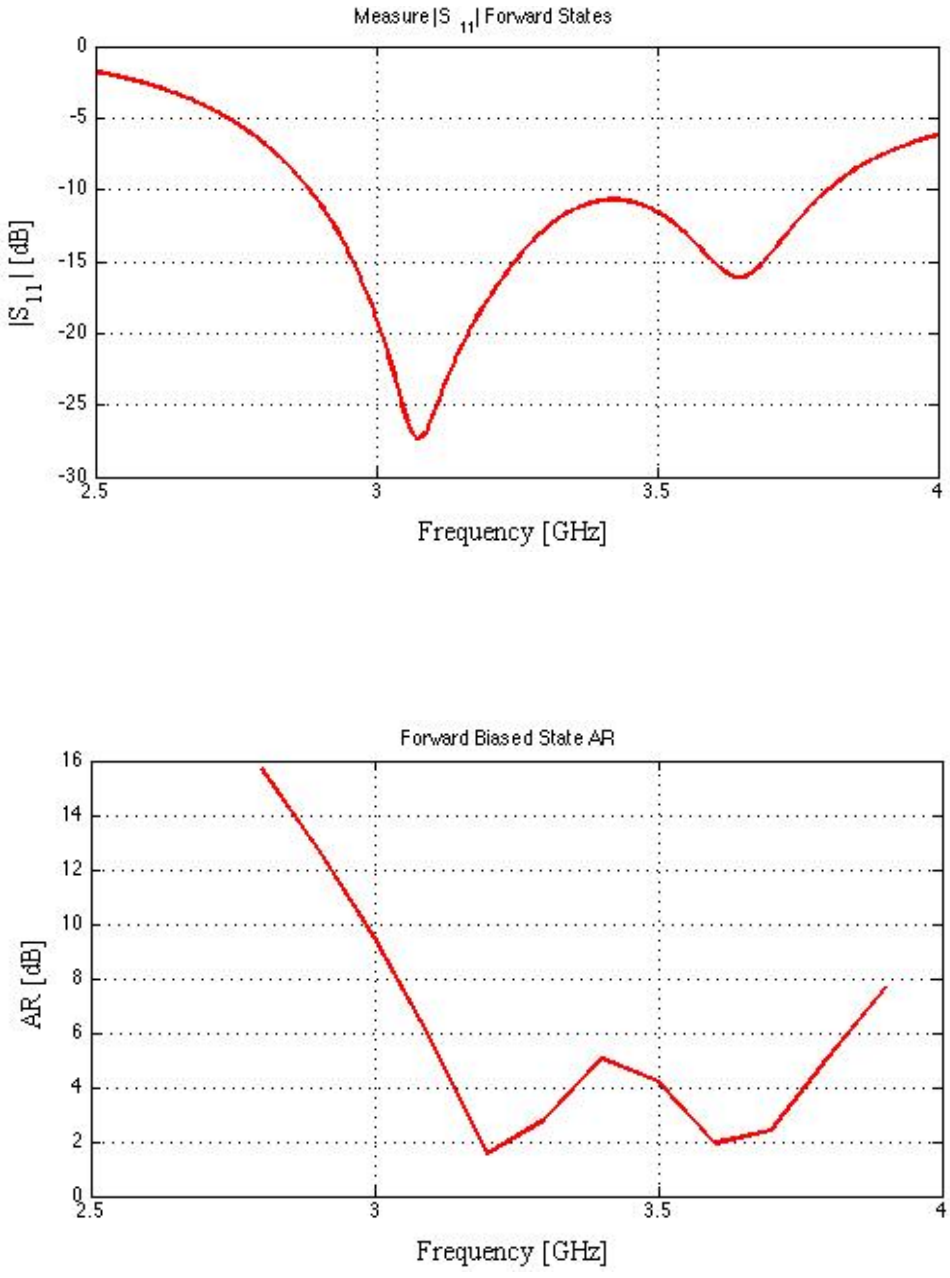

Fig. 3.16: S_{11} (up) and Axial Ratio (down).

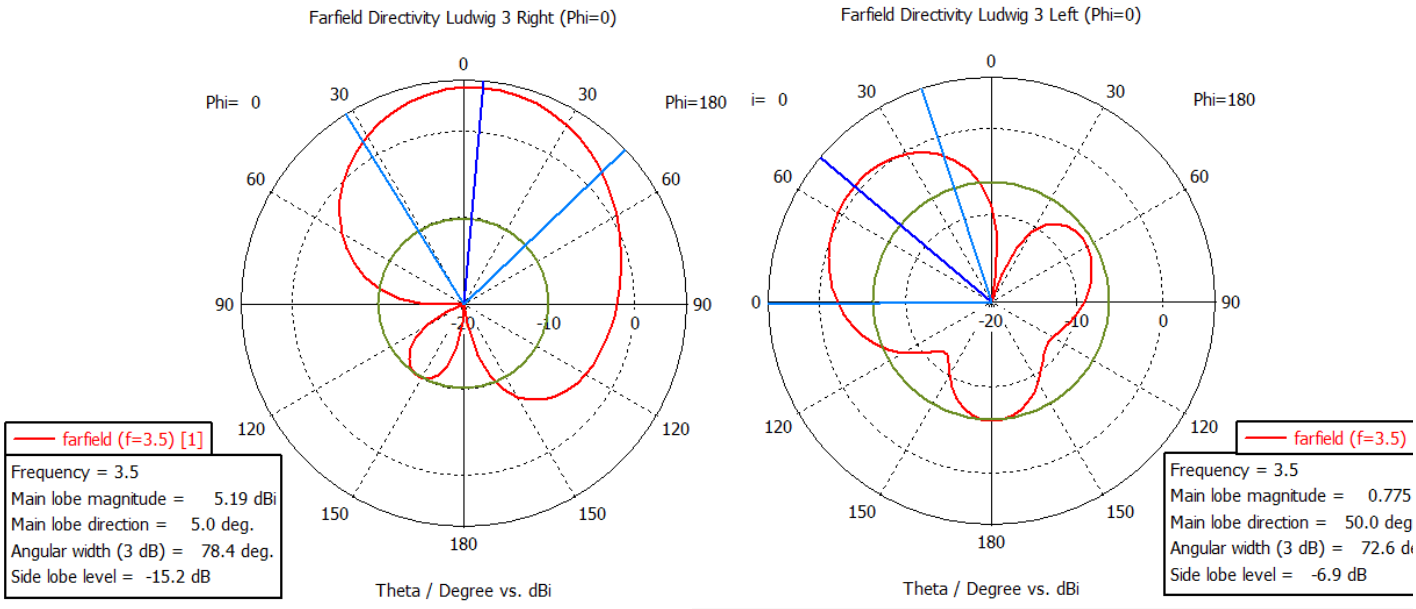

Fig. 3.17: XZ plane Right handed (on the left) and Left handed (on the right) component.

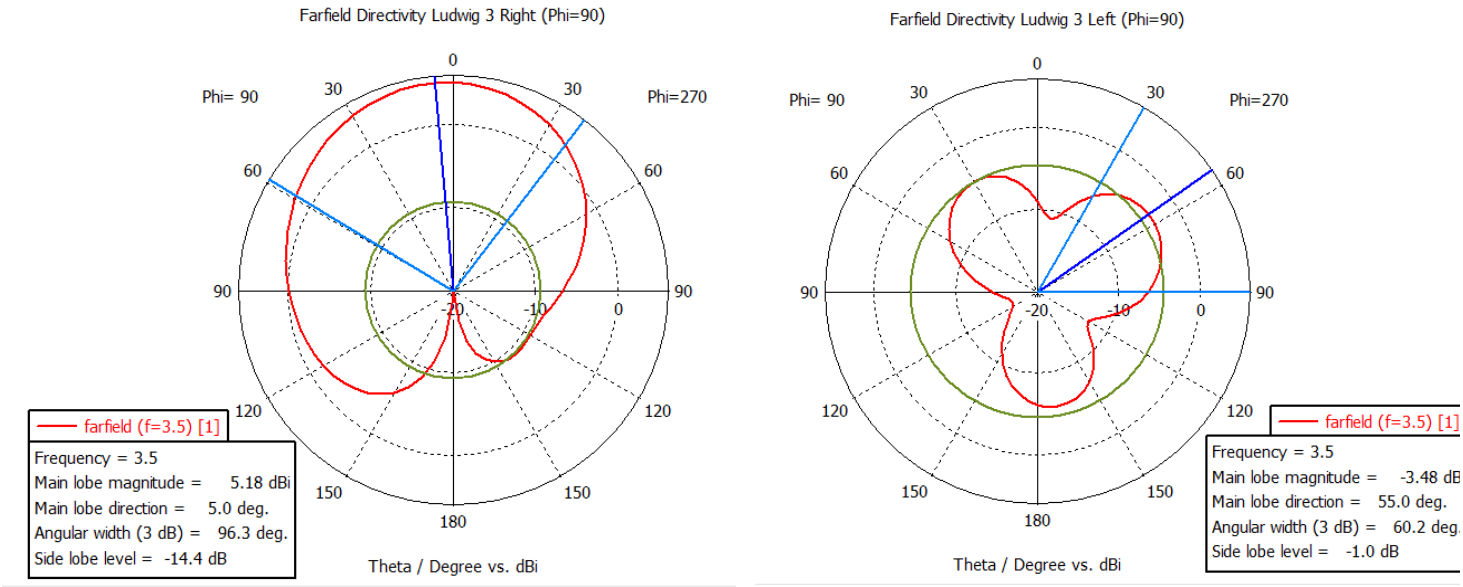

Fig. 3.18: XY plane Right handed (on the left) and Left handed (on the right) component.

Left Hand Circular Polarization

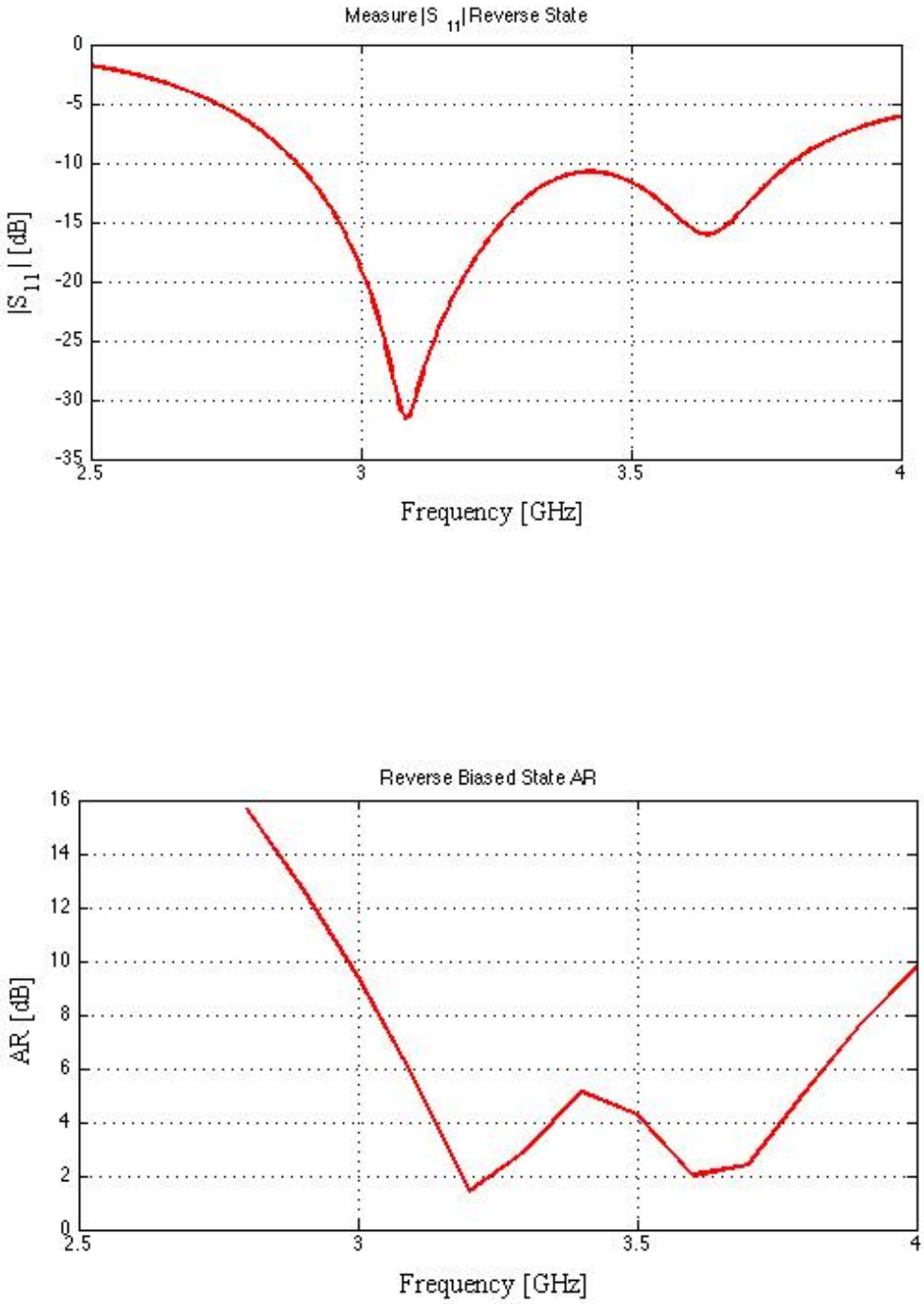

Fig. 3.19: S_{11} (up) and Axial Ratio (down) for the real LHCP antenna.

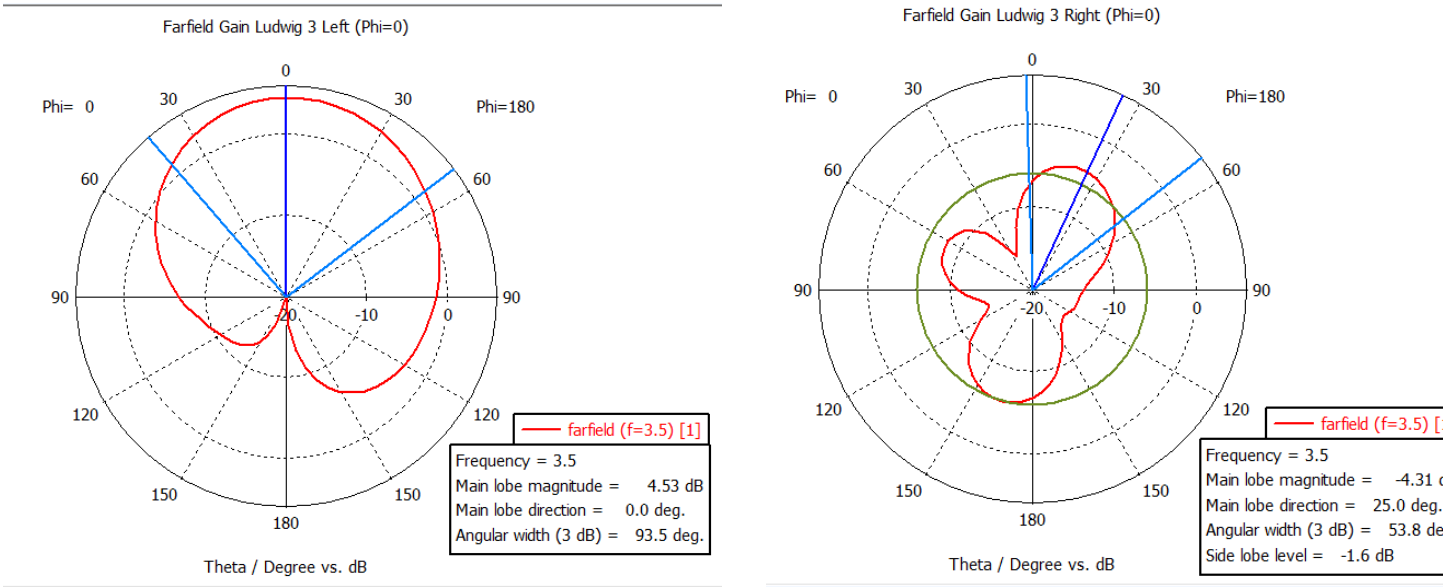

Fig. 3.20: XZ plane Left handed (on the left) and Right handed (on the right) component.

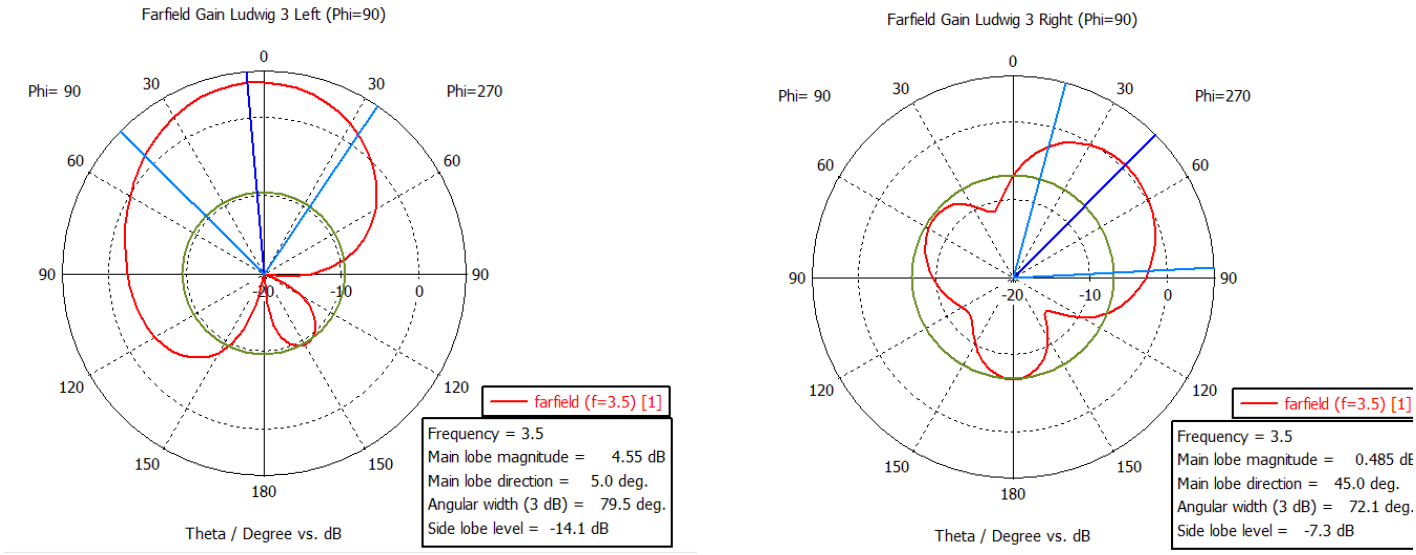

Fig. 3.21: XY plane Left handed (on the left) and Right handed (on the right) component.

3.6 Conclusion

As a proof of concept, a circular polarization switchable antenna has been simulated. From simulations, we conclude that the antenna will be able to switch from right handed circular polarization to left handed circular polarization. The first one exhibits a wide bandwidth in terms of impedance, more than 900 MHz centered around 3.5 GHz, and more than 600 MHz in terms of Axial Ratio. For the symmetry, we expect the same behavior to the left handed circular polarization. In fact, we have more than 700 MHz impedance bandwidth and more than 600 MHz in terms of Axial Ratio.

Chapter 4: Prototypes & Measurements

The first part of this section describes the prototypes fabrication. Then, the measurement results of the design discussed in Chapter 3 are shown.

4.1 Design with Ideal Components

For this kind of design, it has been decided to make ten prototypes in total, six for the right hand circular polarized antenna and other six for the left one. This choice is due to the cork substrate: as said in 3.2.3, it is a non homogeneous material and that's mean that its dielectric properties could change for different prototypes and we want study how this influences the results.

4.1.1 Assembly Process

The assembly process is very simple. It provides to achieve the cavity structure just positioning the tube eyelets with a properly machine, depicted in Fig. 4.1. There are not lumped components, then no soldering is required.

Fig 4.1: Tube eyelets (on the right) and the relative Machine (on the left).

4.2 Design with Lumped Components

Also in this case, six prototypes are made. They have different design as said in Chapter 3, and the assembly process is more complicated because of the necessity to solder the lumped components. The next paragraph describes this process.

4.2.1 Assembly Process

It is possible divide this process in three phases.

PHASE I: P-i-N diodes Solder Process

As said in section 3.5.7, the diodes length is too much small to take in account an hand soldering. Hence, an appropriate oven, called *Reflow Oven,* has been used. This procedure will be discuss in the next section. At the same time, cork and flectron will be cut using a laser cutter and combined together by glue heated using an iron. Fig. 4.2 shows some details of this phase.

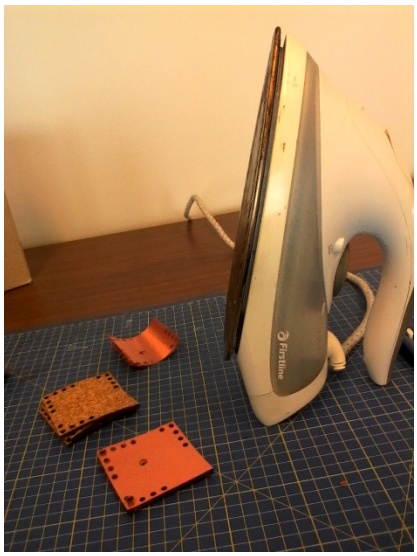

Fig. 4.2: Gluing Flectron on the Cork.

PHASE II: Assembly Structure Process

This phase is the same explained in 4.1.1. Tube eyelets are used to connect the top layer patches with the ground plane. In this way, the cavity structure is achieved, as shown in Fig. 4.3.

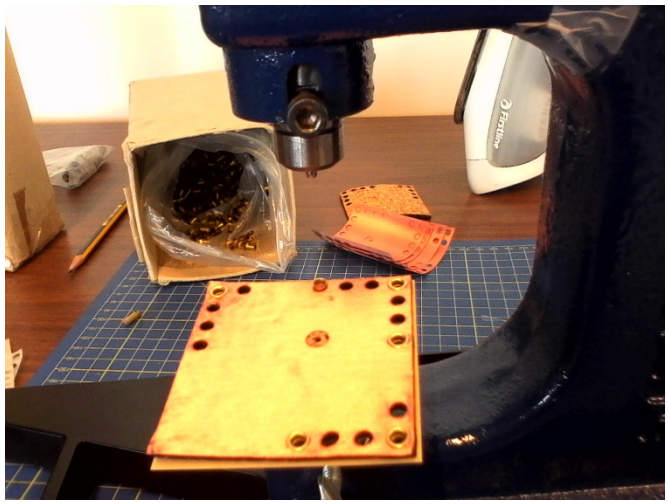

Fig. 4.3: Applying tube eyelets to achieve the cavity structure.

PHASE III: Capacitors Solder Process

The resulting antenna is shown in Fig. 4.4 for ideal components design.

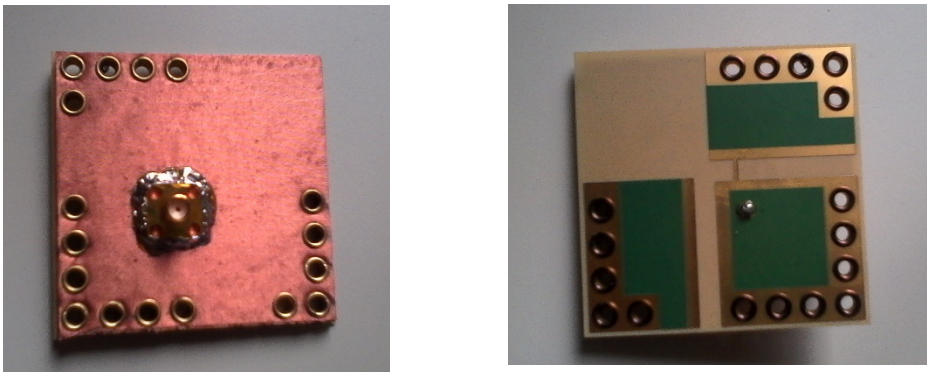

Fig. 4.4: Bottom (left) and Top (right) view of the final antenna with ideal components.

For the prototypes with lumped components, DC blocker capacitors were soldered as well. The choice to solder these components at the end of the entire process is due to their proximity to the tube eyelets. In fact, if they were placed and soldered before Phase II, the related mechanical stress could break their solder points. In both cases, we have to solder the coaxial connector. In particular, the inner conductor to the main patch and the outer conductor to the ground plane. The ground plane is made of a Flectron sheet glued to the cork. Furthermore, for the design with lumped components, we have to solder an inductor through the anular slot.

Reflow Soldering

It is a process in chich a solder paste (a sticky mixture of powered solder and flux) is used to temporarily attach one or several electricalcomponents to their contact pads, after which the entire assembly is subjected to controlled heat, which melts the solder, permanently connecting the joint. Heating may be accomplished by passing the assembly through a reflow oven or under an infrared lampor by soldering individual joints with a hot air pencil. Reflow soldering is the most common method of attaching surface mountcomponents to a circuit board ant its goal is to melt the solder and heat the adjoining surfaces, without overheating and damaging the electrical components.

Reflow Oven

A typical reflow oven is depicted in figure 4.5. The oven contains multiple zones, which can be individually controlled for temperature. Generally there are several heating zones followed by one or more cooling zones. The PCB moves through the oven on a conveyor belt, and is therefore subjected to a controlled time-temperature profile. The heat source is normally from ceramic infrared heaters, which transfers the heat to the assemblies by means of radiation. Ovens which also use fans to force heated air towards the assemblies (which are usually used in combination with ceramic infrared heaters) are called infrared convection ovens.

Fig. 4.5: Reflow Oven.

4.3 Measurements Plan

All the prototypes are made by hand. The cork and the flectron cut, including the holes, is made using a laser cutter. Then they are attacched by glue. Afterwards, the tube eyelets are placed and cavity structure is achieved. In the end, coaxial connectors are soldered. The procedure differences between the two designs are the same discussed above in 4.1.1 and 4.2.1.

First of all, every prototypes with no lumped components are tested and measured. The most important parameters are the S11 and the Axial Ratio, as said in Chapter 2. These parameters are easily to measure and they do not take much time to be measured. Then, we can compare the measured results with the simulated ones.

Afterwards, the prototype with lumped components can be tested and measured. For this purpose, a first complete prototype, with both P-i-N diodes, will be assembly. In this way we could easily compare the results with the simulations because the designs are the same. If it will work as we expect, we will procede to measure the radiation pattern. This procedure takes about one hour, as explained in Chapter 2. Otherwise, if it won't work, we could go back in the design phases with the prototypes left.

For example, we could build one prototype with only the forward biased P-i-N diode, leaving the other footprint unconnected as open circuit. Or we could replace the DC blocker capacitors with wires, as through connections. In any case, all these decision will be made by time.

4.4 Prototypes with Ideal Components

Prototypes with ideal components are useful to verify the geometry in a low complex topology. They also give information on the influence of the substrate and on the fabrication process. As we can see in Fig. 4.6, we can say that the eyelets collapsing and the cork material do not have severe influence.

4.4.1 Right Hand Circular Polarized Antenna

The layout depicted in Fig. 3.8 (on the right) has been fabricated and measured. In Fig. 4.6, the measured performance is compared with the simulation results for the reflection coefficient and axial ratio. As we can see, the parameters are predicted relatively well by the simulation. The antenna shows an impedance bandwidth of about 700 MHz while the AR is also lower than 6 dB in a bandwidth of 600 MHz. The mismatch between simulation and measurement can be related to variations in the fabrication process, for instance, the connector soldering.

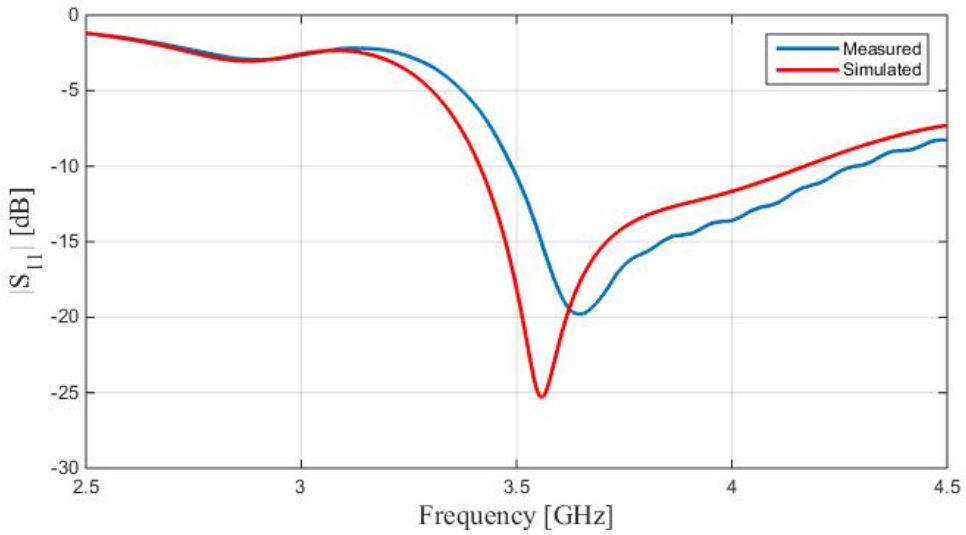

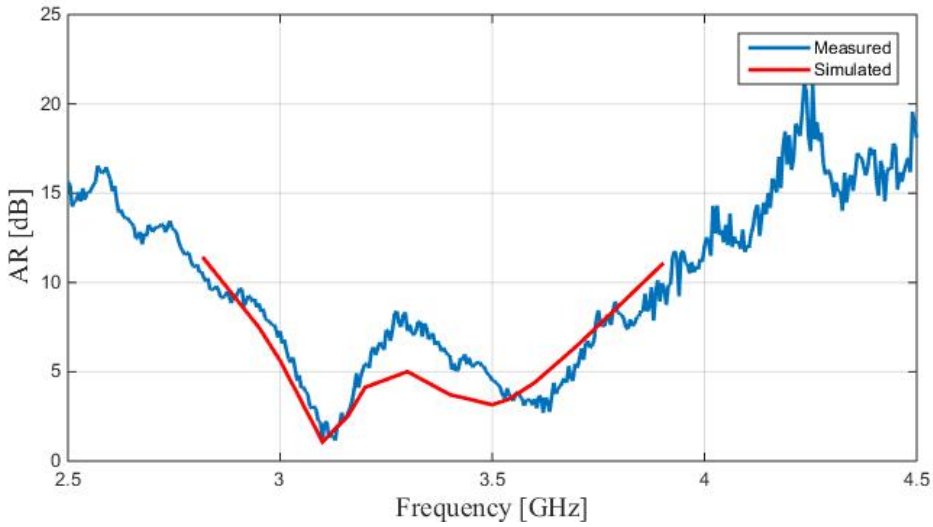

Fig. 4.6: Measured and simulated S_{11} (up) and AR (down) for RHCP prototype.

4.4.2 Left Hand Circular Polarized Antenna

The layout depicted in Fig. 3.8 (on the left) has been fabricated and measured. In Fig. 4.7, the measured performance is compared with the simulation results for the reflection coefficient and axial ratio. Also the left hand circular polarized antenna shows an impedance bandwidth of about 700 MHz while the AR is lower than 6 dB in a bandwidth of 600 MHz.

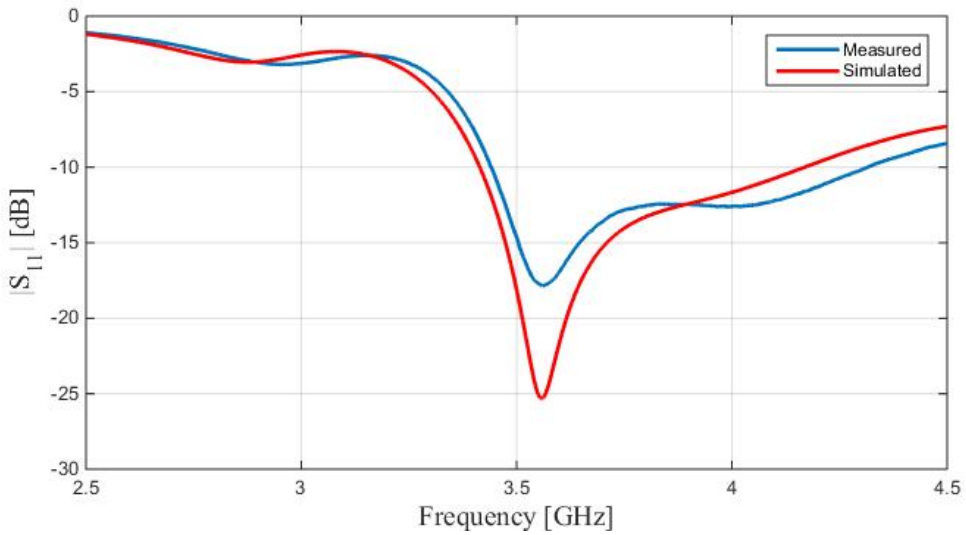

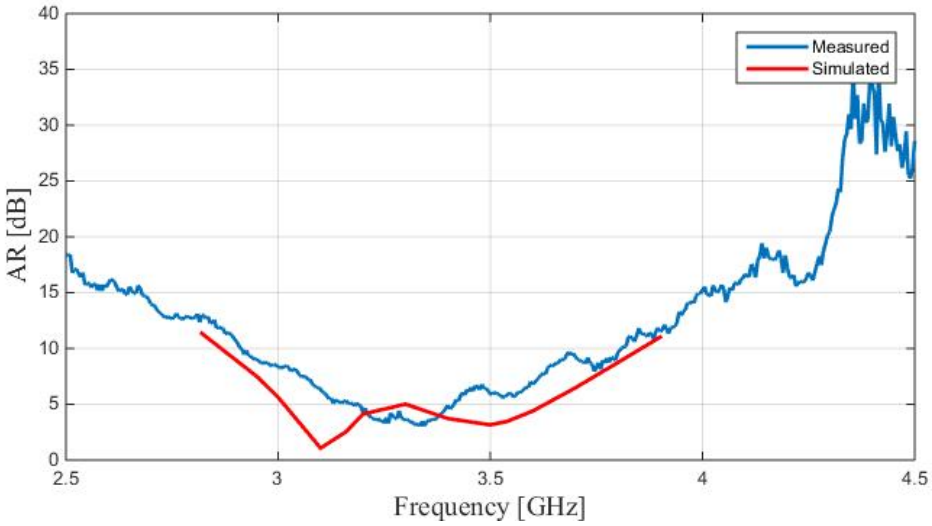

Fig. 4.7: Measured and simulated S_{11} (up) and AR (down) for LHCP prototype.

As seen in section 3.5.2, studying the behavior in a wider frequency range, also the measured S_{11} is well predicted by the simulation, as we can see in the next figure.

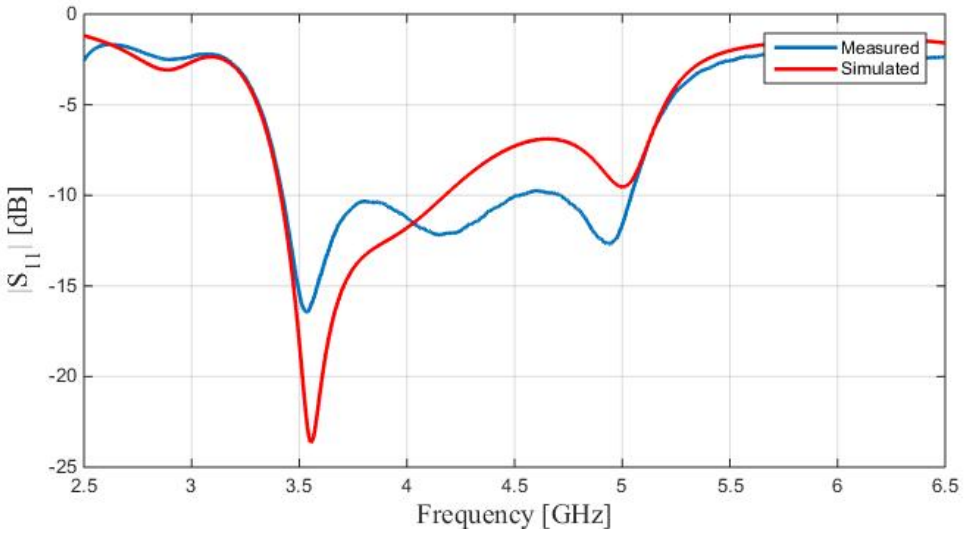

Fig. 4.8: Measured and simulated S_{11} in a wider frequency range.

4.5 Prototypes with Lumped Components

The first measurement results, together with the simulated results, are shown in Fig. 4.9. Introducing lumped components in the design, the antenna performance will be degraded due to the parasitic components effects. Depending on their resonance frequency, we expect a frequency shift around the resonance frequencies and variations of the resonance peaks deepness.

A peak in the S_{11} plot at a certain frequency indicates that something in the design is resonating. In general, we wish that this something is the antenna, that is designed to resonate and hence to radiate at that frequency. This is the case of the two main peaks in Fig. 4.9. Going from prototypes with ideal components to prototypes with lumped components, some extra peaks appear. Seeing that cork material and eyelets collapsing do not influence much the antenna behavior, it is plausible to say that those extra peaks come from the lumped components. The tricky part of introducing lumped components in the design is to model them as best as possible in order to see, during the simulations, how they influence the antenna behavior.

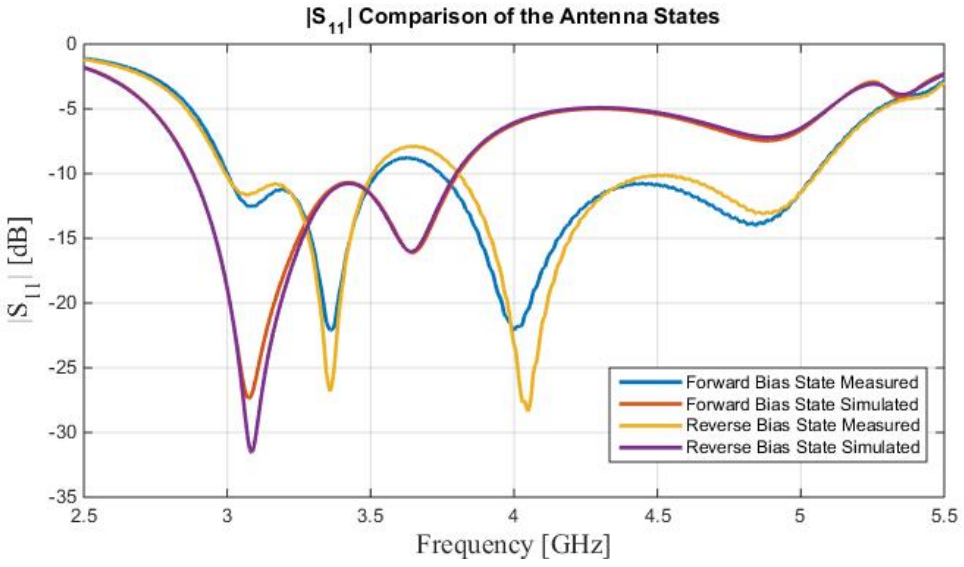

Fig. 4.9: S_{11} comparison of the Antenna States.

In this thesis, a basic modeling of lumped components, particularly for P-i-N diodes, has been made. It is believed that this could be the main reason why we do not have extra peaks in the simulation results and hence the reason why there is that discrepancy between the two curves. At those frequencies the lumped components are resonating and it means that they are absorbing power without radiate, so they are degrading the antenna performances. Other reasons of discrepancy can be related with the soldering procedure. In particular, the capacitors were soldered by hand and this was not very easy because they have small package, see [11].

4.5.1 Right Hand Circular Polarized Antenna

Fig. 4.10 shows the measurements result together with the simulations result. In this case the bias current is positive (forward biased state) and the antenna shows RHCP behavior. Do not taking in account the extra peaks, we can say that the measurements shown the same trend of the simulations with two main peaks, in which the antenna is radiating, a bit upshifted in frequency and not always under -10 dB.

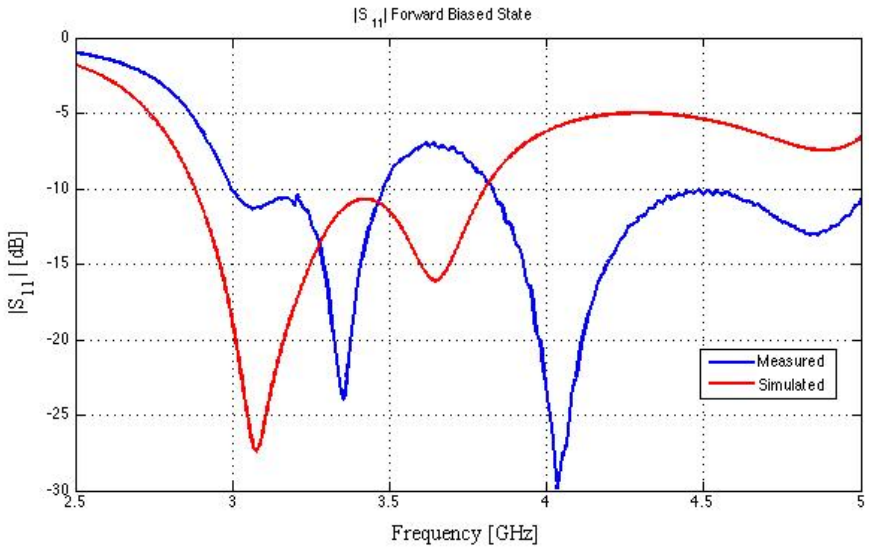

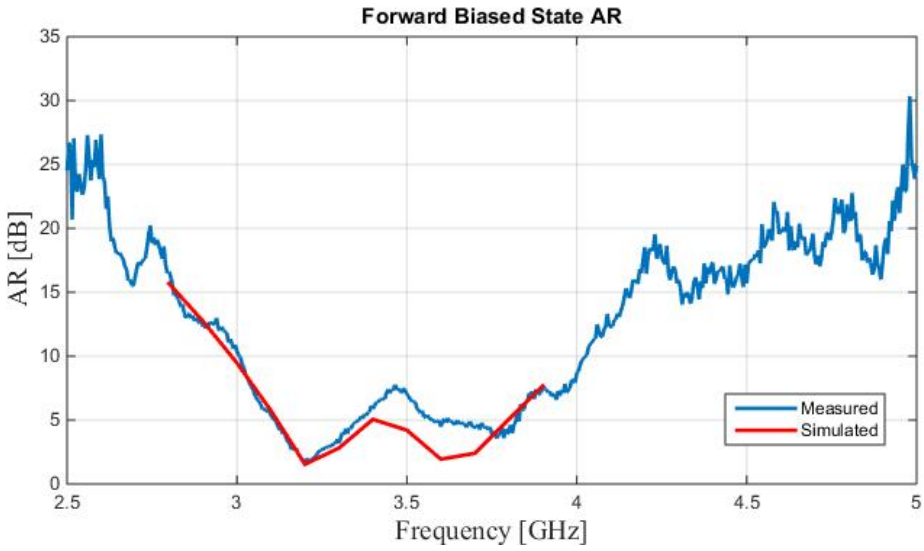

Fig. 4.10: S_{11} and Axial Ratio for the forward biased state.

Looking at the antenna Gain over azimuth angle, we can see from Fig. 4.11 that the maximum value, 5 dB, is along the broadside direction and it is also quite symmetric around this direction. This behavior was expected because in a cavity the maximum value of the E-field is in the center of the cavity itself and it goes down going toward the border. Fig. 4.11 also shows the Gain over frequency for broadside direction and we can see that maximum of 8 dB is around 3 GHz and it oscillates around 5 dB for the others frequencies.

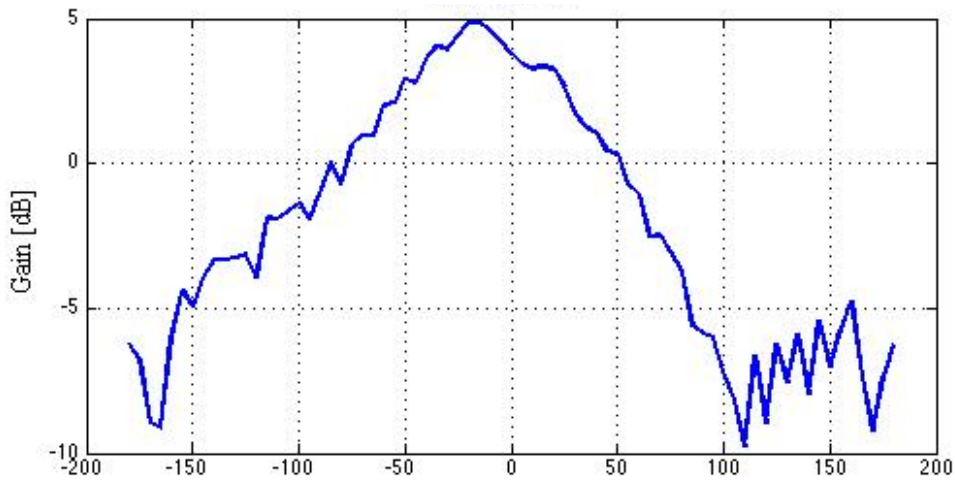

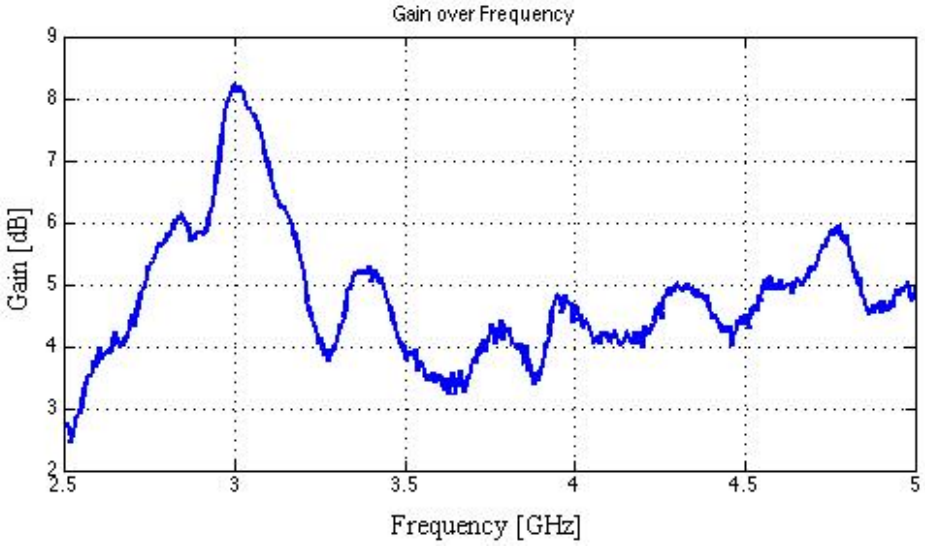

Fig. 4.11: Gain VS Elevation angle (Up) and VS Frequency (down).

4.5.2 Left Hand Circular Polarized Antenna

The compared results are shown in Fig. 4.12. The bias current now is negative (reverse biased state) and the antenna shows LHCP. We can say the same of the previous configuration.

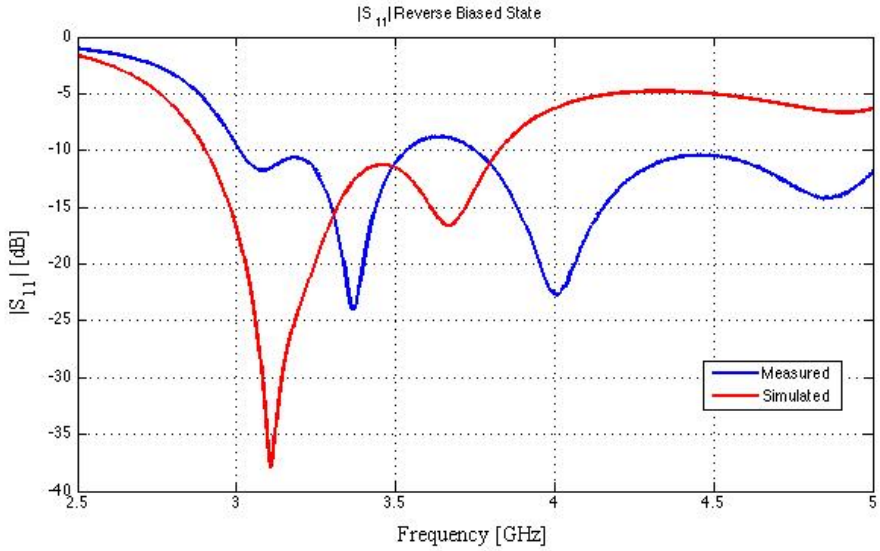

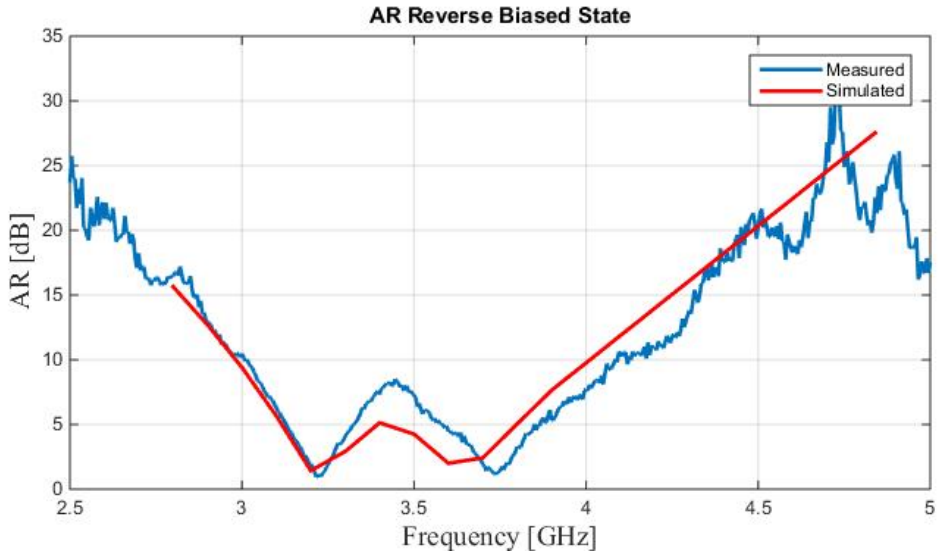

Fig. 4.12: S_{11} and Axial Ratio for the reverse biased state.

As we can see in Fig. 4.13, also in this case, thanks to the symmetry of the antenna, the Gain trend is almost the same as the previous configuration both in frequency and azimuth.

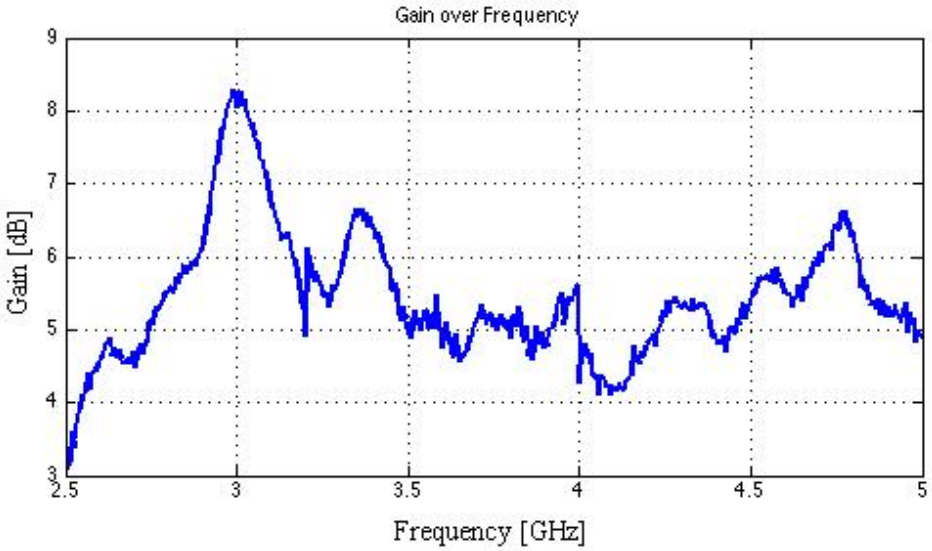

Fig. 4.13: Gain VS Elevation angle (Up) and VS Frequency (down).

In both cases, after what we said in section 4.5, the simulations predict well the measurements. It is believed that the remaining discrepancy between the curves is due to manual manufacturing inaccuracies. The antenna exhibits much more than 500 MHz of bandwidth that is the minimum value to define the antenna as UWB antenna. However we have to say that even if the bandwidth goes from 3.1 GHz up to beyond 5 GHz, the real bandwidth in which the antenna behavior is the expected, goes from 3.1 GHz up to almost 4.5 GHz in terms of S_{11} impedance bandwidth at -10 dB. In these frequency range the minimum S_{11} value is -8 dB that could be enhanced with better simulation. Get the required axial ratio bandwidth is the tricky part of the design because achieving wide bandwidth is not simply. In terms of axial ratio the antenna exhibits around 700 MHz of bandwidth, from 3.1 GHz up to 3.8 GHz, even if it is not always under 6 dB in the mentioned frequency range that could be also acceptable considering the novelty of the antenna.

Chapter 5: Conclusion & Future Work

Regarding the prototypes with ideal components, we can say that have a lower complexity design, and geometry, was useful to verify the switching concept as first step of the project. Furthermore, it led to a good matching between simulations and measurements. The results have shown that the hand-made fabrication process is relatively easy and it does not influence much the antenna performances.

Regarding the prototypes with lumped components, as we saw in previous sections, we can say that an accurate modeling of them is needed to predict well the measurements. They could introduce extra resonant peaks and hence wasting power. We also have to say that the hand-made fabrication process, concerning the soldering, is more difficult because the capacitors are very small. This could lead to have different soldering points for the capacitors on the same prototype and also for different prototypes, hence could lead to have different measurements for different prototypes with the same topology.

Anyway, the polarization reconfigurability in a huge bandwidth has been proven for both prototypes, with ideal and lumped components, for an UWB antenna.

Future work should be focused on finding an accurate model for the P-i-N diodes in order to make more realistic the simulations. The same is for the capacitors.

Furthermore, a mechanical fabrication process could lead to better results.

Thanksgiving

In the end of this Telecommunications engineering degree course (Bachelor and Master), I feel the need to say thanks to some people.

First of all, my parents, Mrs **Nuccia** and Mr **Tenente**, thanks to their continuous and unceasing (sometimes excessive) encouragements, they have always kept me on what would have been the right direction towards the achievement of today. The light in their eyes gave a meaning to all the sleepless nights spent in the glow of a lampshade and to all the anxiety sweated in classrooms in Via Dio ti Salvi. Along with them, my brother **Kat** and my little sister **Nairobi**, always close at the right moment even if physically far. My blood brother, **Luigi**, always ready with business ideas never realized. Do not worry: one day we will find the winning one!

Thaks to my dear made in Tuscany friend **Matteo**, for the thousand Skype calls started to solve important issues about modulations, encodings, laser and much more but often ended talking about the problems that afflict humanity. And how I cannot mention my Philarmonic brother **Mario**, *Lo Zio* for friends, thanks to which my attitudes as musician, often (and gladly) equivocate, they reached the fame of such a high level that it becomes even legend for the Pisan streets.Thanks to her who supported me and especially tolerated me in these 18 months, **Sabrina**, for having been close in extra university moments and to be, still, an inspiration for personal improvements. Thanks Honey. Still a little time for our Teddy (bau bau). Furthermore, I want to say thank you to: **Rafda**, the only one who understand my style of jokes, the great **Pazza**, unique and valuable companion of battles to conquer the laws of physics that govern electromagnetism, **Nino**, for teaching me the English formulas, **Milad**, for inventing the term "*dispunti"* to indicate a mix of handouts and notes, the supreme Master **Luca**, a source of daily inspiration and driver of afternoons in Pacinotti, my flatmates, **Bruno**, **Salvo**, **Ilaria** e **Sara**, four intense months of old women from Bari, my family from Sardinia, **Agostino, Simone, Baingiu Sr., Baingiu Jr., Montesu, Valeria e Helena,** to explain me the differences between people from Ottana and people from Orgosolo. Last but not least: **Matteo**, **Gianluca**, **Selenia**, **Paola**, **Federica**, **Alessio**, **Stefano**, **Luigi**, **Davide**, **Giorgio**, **Giuseppe**, **Mario**, **Piera** Mezzogiorno, **Lucia**, **Michele**, **Francesco** and all others who now are not in my mind, but I have to deliver the thesis so it is enough (smile).

Passing on the other side of the desk of the University of Pisa, I would like to thank personally my advisor, Prof. **Paolo Nepa**, for giving me the opportunity to spend a period of training abroad and have always been interested in my work, but above all, for your efforts in getting all the documents, signatures and various stamps, required for the departure. A sincere thanks to Ing. **Andrea Michel**, for having been always present in these months and interested in a particular and sincere way to my work. You are a friend.

Coming at the University of Ghent, I would like to thank my advisor, Prof. Dr. Ir. **Hendrik Rogier**, for welcoming me into his lab and have always been a person friendly and helpful. Along with him, Ir. **Sam Agneessens**, for introducing me to the CAD design and teaching me the fastest and effective ways to solve problems related to it. Thanks also to Ir. **Sam Lemey**, for the time spent to explain me how to manage and set an anechoic chamber and all the related instrumentation for the prototypes measurements. To all three, a final thanks for reviewing and correcting the present thesis.

Ringraziamenti

Alla fine di questo percorso di Laurea in Ingegneria delle Telecomunicazioni (triennale e magistrale), mi sento in dovere di ringraziare alcune persone.

Prima di tutti, i miei genitori, la signora **Nuccia** e il signor **Tenente**, che grazie ai loro continui e instancabili (a volte eccessivi) incoraggiamenti, mi hanno sempre mantenuto su quella che sarebbe stata la giusta direzione verso il traguardo raggiunto oggi. La luce nei loro occhi ha dato un significato a tutte le notti insonni passate al chiarore di una abat-jour e a tutta l'ansia trasudata nelle aule in Via Dio ti Salvi. Insieme a loro, mio fratello **Kat** e la mia sorellina **Nairobi**, sempre vicini al momento giusto anche se fisicamente lontani. Il mio amico fraterno, **Luigi**, sempre pronto con idee di business mai realizzate. Non preoccuparti: un giorno troveremo quella vincente! Grazie al mio caro amico made in Tuscany **Matteo**, per le mille mila Skypate iniziate per risolvere questioni importanti su modulazioni, codifiche, laser e quant'altro ma spesso finite a parlare dei problemi che affliggono l'umanita'. E come non citare il mio fratello Filarmonico **Mario**, alias *Lo Zio*, grazie al quale le mie attitudini musicali, spesso (e volentieri) equivocate, hanno raggiunto una fama di livello cosi' alto da diventare addirittura leggenda per le vie pisane. Grazie a colei che mi ha supportato e soprattutto sopportato in questi 18 mesi, **Sabrina**, per essermi stata vicino in momenti extra univeristari e per essere, ancora oggi, ispirazione di miglioramento personale. Grazie Amore. Manca poco per il nostro Teddy (bau bau). Inoltre voglio ringraziare: **Rafda**, unica spalla di supporto per le battute alla Cyrano de Bergerac, il grande **Pazza**, unico e validissimo compagno di battaglie per la conquista delle leggi della fisica che regolano l'elettromagnetismo, **Nino**, per avermi insegnato le formule in inglese, **Milad**, per aver coniato il termine *"dispunti"* atto ad indicare un mix tra dispense e appunti, il sommo Maestro **Luca**, fonte di ispirazione quotidiana e trascinatore di pomeriggi in Pacinotti, i miei coninquilini, **Bruno**, **Salvo**, **Ilaria** e **Sara**, quattro mesi intensi tra le vecchie baresi, la mia famiglia Sarda, **Agostino, Simone, Baingiu Sr., Baingiu Jr., Montesu, Valeria e Helena,** per le precisazioni su quelli di Ottana e quelli di Orgosolo. E ancora: **Matteo**, **Gianluca**, **Selenia**, **Paola**, **Federica**, **Alessio**, **Stefano**, **Luigi**, **Davide**, **Giorgio**, **Giuseppe**, **Mario**, **Piera** Mezzogiorno, **Lucia**, **Michele**, **Francesco**, e tutti gli altri che ora non mi vengono in mente ma devo consegnare la tesi quindi basta cosi' (smile).

Passando dall'altro lato della cattedra dell'Universita' di Pisa, vorrei ringraziare in prima persona il mio relatore, Prof. **Paolo Nepa**, per avermi dato la possibilita' di trascorrere un periodo di formazione all'estero e per essersi sempre interessato al mio lavoro, ma soprattutto per essersi impegnato nell'ottenere tutti i documenti, firme e timbri vari, necessari per la partenza.
Un sincero ringraziamento all' Ing. **Andrea Michel**, per essermi stato sempre presente in questi mesi interessandosi in modo particolare e sincero al mio lavoro. Sei un amico.

Venendo all'Universita' di Ghent, vorrei ringraziare il mio relatore, Prof. **Hendrik Rogier**, per avermi accolto nel suo laboratorio e per essersi sempre dimostrata una persona cordiale e disponibile. Insieme a lui, l' Ing. **Sam Agneessens**, per avermi introdotto alla progettazione CAD ed avermi insegnato i modi piu' veloci ed efficaci per risolvere problemi legati alla stessa.
Un grazie anche all' Ing. **Sam Lemey**, per il tempo passato a spiegarmi come gestire e settare una camera anecoica e tutta la strumentazione annessa per la misurazione dei prototipi. A tutti e tre un ringraziamento finale per aver revisionato e corretto la presente tesi.

BIBLIOGRAPHY

[1] Olivier Caytan, Sam Lemey, Sam Agneessens, Dries Vande Ginste, Piet Demeester, Caroline Loss, Rita Salvado, Hendrik Rogier, *"Half-Mode Substrate-Integrated- Waveguide Cavity-Backed Slot Antenna on Cork Substrate"*

[2] Olivier Caytan, Sam Agneessens, Sam Lemey, Dries Vande Ginste, Piet Demeestery, Hendrik Rogier, *"Ultra-wideband Cork Substrate-Integrated-Waveguide Cavity-Backed Slot Antenna"*

[3] D. Dardari, R. D'Errico, C. Roblin, A. Sibille, M. Win, *"Ultrawide Bandwidth RFID: The Next Generation?"*, Proceedings of the IEEE, vol. 98, no. 9, September 2010.

[4] Xue-Xia Yang*, Bo Gong, Guannan Tan, Zhongliang Lu, "*Reconfigurable Patch Antennas With Four-Polarization States Agility Using Dual Feed Ports",*School of Communication and Information Engineering, Shanghai University

[5] G. Q. Luo and L. L. Sun*, "A reconfigurable Cavity backed antenna for circular polarization diversity",* microwave and optical technology letters, vol. 51, no. 6, pp 1491- 1493, 2009

[6] Alexander Vindelinkx, "*Reconfiguration of wearable antennas through feed-line bias*", Master thesis, Ghent University, 2015

[7] M. Bozzi, A. Georgiadis, and K. Wu, *"Review of substrate-integrated waveguide circuits and antennas",* IET Microwaves, Antennas & Propagation, vol. 5, no. 8, June 2011.

[8] S. P. Silva, M. A. Sabino, E. M. Fernandes, V. M. Correlo, L. F.Boesel, R. L. Reis, *"Cork: properties, capabilities and applications"*, International Materials Reviews, Maney Publishing, vol. 50, pp. 345 365, 2005.

[9] MACOM technology solution MA4AGBLP912 PiN diode.

[10] L. Silvestri, *"Design of Reconfigurable Textile Substrate Integrated Waveguide"*, Master thesis, Ghent University 2014

[11] AVX-RF Accu-P thin-film capacitors for RF signals and power applications.

[12] A. petosa, *"An Overview of Tuning Techniques for frequency agile antennas"*, IEEE Antenna and propagation magazine, vol 54, no 5, pp 271-296, 2012

[13] V. Sekar, M. Armendariz, K. Entesari, *"A 1.2-1.6 GHz substrate-integrated-waveguide RF MEMS tunable filter",* IEEE transactions on Microwave theory and techniques, vol 59, no 4, 2011

[14] Agilent technology, "*Understanding RF/Microwaves solid states switches and their applications"*, May 2010

[15] D. M. pozar, "*Microwave Engineering*", Wiley, 2012

[16] Liang Wu, "*Substrate integrated waveguide antenna applications*", PhD thesis, Kent university, august 2015.

[17] Bozzi, Perregrini, Wu, Arcioni, "*Current and future research trends in SIW technology",*
Univeristy of Pavia, IEEE, radioengineering, vol 18, no 2, June 2009

[18] Khidre, Lee, Tang, Elsherbeni, "*Circular polarization reconfigurable wideband E shaped patch antenna for wireless applications"*, IEEE transactions on antenna and propagation, vol. 61, no 2, February 2013

[19] Joshua M. Kovitz and Yahya Rahmat-Samii, "*Enhanced Broadband Performance of Thick CP Patch Antennas: A Novel Annular Gap Capacitor Design"*, Electrical Engineering Deparment, University of California Los Angeles, 2014

[20] Jeen-Sheen Row and Jia-Feng Wu, "*Aperture-Coupled Microstrip Antennas With Switchable Polarization"*

[21] Ahmed Khidre, Kai-Fong Lee, Fan Yang, and Atef Z. Elsherbeni, "*Circular Polarization Reconfigurable Wideband E-Shaped Patch Antenna for Wireless Applications*"

[22] Y. J. Sung, "*Reconfigurable Patch Antenna for Polarization Diversity*"

[23] Kyungho Chung, Yongsik Nam, Taeyeoul Yun, and Jaehoon Choi, *"Reconfigurable Microstrip Patch Antenna with Switchable Polarization"*.

[24] Texas Instruments, LM134/LM234/LM334 3-terminal adjustable current source, May 2013

[25] http://www.antenna-theory.com/measurements/antenna.php#equipment

[26] http://www.cisco.com/c/en/us/products/collateral/wireless/aironet-antennas-accessories/prod_white_paper0900aecd806a1a3e.pdf

[27] Michael D. Foegelle, "*Antenna Pattern Measurement: Conceps and Techniques"*, Compliance Engineering

[28] Xue-Xia Yang, Bo Gong, Guannan Tan, and Zhongliang Lu, "*Reconfigurable Patch Antennas With Four-Polarization States Agility Using Dual Feed Ports*",
School of Communication and Information Engineering, Shanghai University

[29] Kyungho Chung, Yongsik Nam, Taeyeoul Yun, and Jaehoon Choi "*Reconfigurable Microstrip Patch Antenna with Switchable Polarization"* ETRI Journal, Volume 28, Number 3, June 2006

[30] Joshua M. Kovitz, Yahya Rahmat-Samii, "Using Thick Substrates and Capacitive Probe Compensation to Enhance the Bandwidth of Traditional CP Patch Antennas", IEEE TRANSACTIONS ON ANTENNAS AND PROPAGATION, VOL. 62, NO. 10, OCTOBER 201

List of Figures and Tables